FABRICATION AND CHARACTERIZATION OF LIQUID ELECTROLYTE GATED POLYMER FIELD EFFECT TRANSISTOR FOR BASIC CIRCUIT APPLICATIONS

by

Berkan Yaman

B.S., Electrical and Electronics Engineering, Boğaziçi University, 2010

Submitted to the Institute for Graduate Studies in
Science and Engineering in partial fulfillment of
the requirements for the degree of
Master of Science

Graduate Program in Electrical and Electronics Engineering Department
Boğaziçi University

2013

ACKNOWLEDGEMENTS

I would like to thank my supervisor Assoc. Prof. Şenol Mutlu for his suggestions, encouragements and helpful behavior. His optimism and solution oriented perspective was a great driving force in the Project.

I would also thank you my Project partner İsmail Terkeşli for his friendship and comprehension, it was a pleasure to be on the same team with him. I would like to express my sincere gratitude to Kader Merve Türksoy for her constant support, she always make me cheer with her lively personality.

Additionally, I would like to thank my friends Gökhan Hacıahmetoğlu, Barış Esen and İsmail Kara for creating an entertaining graduate life. My thanks are extended to whole team of Boğaziçi University Beta Laboratory.

Finally, special thanks go to my parents Suat Yaman and Nazire Yaman. I am grateful to my little brother Tahsin Serkan Yaman for his helpful and considerate behaviour.

This study is fully supported by Turkish Scientic and Technological Research Council (TUBITAK) under the Project number 110E063.

ABSTRACT

FABRICATION AND CHARACTERIZATION OF LIQUID ELECTROLYTE GATED POLYMER FIELD EFFECT TRANSISTOR FOR BASIC CIRCUIT APPLICATIONS

In this thesis, a simple polymer field effect transistor structure is designed and fabricated. To decrease the operating voltage of the transistor, electrolyte solutions are used as gate material. Using electrolyte at the gate increased the capacitance of the induced channel by the effect called electrical double layer formation which allowed transistor to operate under 1V. In the first step DI water is used as electrolyte solution because of its application simplicity. In order to stabilize the gate electrode and create a solid structure for the circuit design a novel electrode framework which is named planar gate electrode structure is implemented. Then, length of the channel is adjusted to be able to analyze the functional polymers that has been synthesized Chemistry Department of the Project. Comparison of different transistor designs has shown that a certain extent of ionic concentration results in higher ionization rate, so increase in the transconductance of the transistor. After the comparison of transistors which are prepared by commercial P3HT and P3HT with hydrophilic functionalization (P3HT-co-P3PEGT), it has also been observed that hydrophilicity of the polymer increases the effect of electrical double layer capacitance. In the last section, a high gain inverter is achieved by integration of P3HT-co-P3PEGT and 100mm NaCl solution. Thus, it is proved that the fabricated OFETs in this study can drive basic digital circuit applications.

ÖZET

TEMEL DEVRE UYGULAMALARI İÇİN SIVI ELEKTROLİT KAPILI POLİMER İNCE FİLM TRANSİSTÖRLERİN ÜRETİMİ VE İNCELENMESİ

Bu tezde, basit bir yapıya sahip elektrolit kapılı polimer ince film transistör tasarlanmış ve üretilmiştir. Transistörün çalıştığı potansiyel gerilim aralığını düşürmek için kapı yalıtkanı olarak elektrolit çözeltisi kullanılmıştır. Bu durum elektriksel çifte katman etkisi sayesinde kanalı indükleyen kapasitansın artmasını sağladı. Transistör bu sayede 1 volt ve altındaki potansiyel gerilimlerde çalışabilir duruma geldi. Uygulama basitliğinden dolayı ilk aşamada kapı elektroliti olarak saf su kullanıldı. Devre tasarımı için entegre bir transistör ve elektrot yapısı gerekir. Bu yüzden yenilikçi bir tasarım olan yüzeysel kapı electrodu tasarımı geliştirildi. Daha sonra projenin kimya departmanı tarafından hazırlanan sentezlenmiş polimerleri deneyebilmek için kanal uzunluğu 4 mikrometreye düşürüldü.. Değişik transistör yapılarının ölçüm sonuçlarının karşılaştırılmasına göre, belli bir derişime sahip elektrolit çözeltilerin daha hızlı iyonizasyon sağladığı tespit edildi. Ticari amaçlı P3HT ve hidrofilik fonksiyona sahip P3HT-co-P3PEGT polimerleri ile üretilen transistörlerin karşılaştırılması sonucunda, hidrofilik özelliğin elektriksel çifte katman kapasitansını arttırdığı belirlendi. Son bölümde, P3HT-co-P3PEGT ve 100 milimolar NaCl çözeltisi ile yüksek kazançlı invertör elde edildi. Böylece, bu çalışmada üretilen transistörün sayısal devreleri sürebilecek fonksiyonelliğe sahip olduğu kanıtlandı.

TABLE OF CONTENTS

LIST OF FIGURES

LIST OF SYMBOLS

g_m	Transconductance
I_D	Drain Current
μ_{linear}	Mobility in Linear Region
$\mu_{saturation}$	Mobility in Saturation Region
V_{DS}	Potential Difference between Drain and Source
V_{GS}	Potential Difference between Gate and Source

LIST OF ACRONYMS/ABBREVIATIONS

EDL	Electrical Double Layer
EDLC	Electrical Double Layer Capacitance
Eg	Energy Bandgap
EGOFET	Electrolyte Gated Organic Field Effect Transistor
FET	Field Effect Transistor
HOMO	Highest Occupied Molecular Orbital
ISOFET	Ion Sensitive Organic Field Effect Transistor
LUMO	Lowest Unoccupied Molecular Orbital
MEMS	Microelectromechanical Systems
MIS	Metal-Insulator-Semiconductor
NaCl	Sodium Chloride
OECT	Organic Electrochemical Transistor
OFET	Organic Field Effect Transistor
OLED	Organic Light Emitting Diodes
P3HT	Poly(3-hexyl)thiophene
PEG	Poly(ethy1ene-glycol)
PMOS	P-type Metal-Oxide-Semiconductor
RFID	Radio Frequency Identification
SiO_2	Silicon Dioxide
UV	Ultraviolet
VTC	Voltage Transfer Curve

INTRODUCTION

1.1. Inorganic Electronics to Polymer Electronics

Today transistors which are made of inorganic semiconductor materials are dominating the industry of electronics, which started with the construction of the first transistor in 1947. Inorganic transistors are in every electronic equipment, such as computers, televisions, phones and vehicles. Nowadays, modern transistor and circuit fabrication become increasingly more complex resulting in higher cost of production. Besides, their poor mechanical flexibility is also an obstacle for their use on applications requiring flexible substrates.

Polymer and organic materials had a strong influence in the research of modern electronics because of their relatively low cost, ease of production and unique functions. After the discovery of conjugated organic and polymer materials, a new class of materials is defined that have the optical and electronic properties of semiconductors. Due to their processing advantages and mechanical properties, organic and polymer semiconducting and conducting materials created a research field which resides between chemistry, physics and electronic engineering that is called organic electronics [1].

One of the main advantages of using polymers in electronics is that they can be processed in solution. Thus, it is possible to use conventional printing techniques that allows large area, high volume and low-cost applications. Producing a silicon chip generally takes weeks of work in ultra clean environment. However, production of organic devices is faster and can be less sophisticated. In addition, organic devices can be integrated monolithically with other organic or polymeric devices such as sensors, actuators and microfluidic devices. Since they can be fabricated on flexible and very thin substrates, the overall system can be flexible and light [2]. They have unique device behaviors that can be useful for different applications [3].

Organic materials are not crystalline solids but amorphous or polycrystalline materials. Thus, charge transport is very slow compared to the the mechanisms in single

crystalline inorganic semiconductor devices. Polymer chips probably cannot be as fast or as miniaturized as their silicon counterparts. It seems unlikely for polymer transistors to replace the silicon ones in a microprocessor. But they may be successfully employed as e-textiles, e-paper, displays, photovoltaics, radio-frequency identification (RFID) tags and security tags [4-5]. The aim of organic electronics is to find an application for the existant materials or to create a material that has optimized properties for a certain application.

A wide variety of organic semiconductor devices has been developed such as, organic light-emitting diodes (OLEDs), solar cells, sensors and organic thin film transistors [6]. This thesis focuses on a particular type of organic thin film transistor which is commonly referred as electrolyte-gated organic field effect transistors.

1.2. Objective and Outline

Organic field-effect transistors (OFETs) are promising for printed electronics in many applications such as chemical sensors, digital logic, RFID tags and displays [7]. P- and n-channel operations are demonstrated in OFETs, thus suggesting the possibility to built complementary circuits [8]. However, a wide range of applications of printed organic electronics get power either from printed batteries, solar cells or via electromagnetic induction [9]. These power sources can generally supply voltage levels ranging from 1V to only a few volts at a current often limited to less than 1 mA [10].

In conventional organic field-effect transistors, low-voltage operation can only be achieved by using gate insulators with high capacitance density. In order to operate at voltage levels of 1 V, 2 V or below OFET must employ nanometer-thick gate insulator layers [11] with a high dielectric constant. However, ultra thin layers are impractical to use in printed electronics where robustness is a major challenge. Thus, the development of printed electronics is facing a great challenge by the lack of transistors and logic circuits that can operate at low voltages and run at high signal speeds. A smart approach to solve this problem is to use electrolytes as the gate insulator material. Electrolytes are commonly used to achieve very high capacitance levels in electrolytic capacitors [4]. In electrolyte-based OFETs, the capacitance which is created by migrated ions at the polymer surface is virtually independent of the thickness of the bulk of the electrolyte layer. This property

makes electrolytes very attractive for use in organic electronic circuit applications [8,12]. This high capacitance is realized by the phenomenon called electrical double layer (EDL) formation and the capacitance is named electrical double layer capacitance (EDLC). Using an ion-conducting electrolyte as an OFET gate dielectric, it has been shown that the formation of EDLs at interfaces can be exploited to induce a very high charge carrier density in the channel of an OFET at low applied voltages [13]. Detailed information about EDL formation is given in Chapter 2.

In this study, we have built an electrolyte-gated organic thin film transistor by using P3HT as the semiconductor polymer. Our aim is to work with aqueous solutions because of several reasons. Firstly, conductivity of liquid electrolytes is higher in several order of magnitude than the conductivity of solid electrolytes [2]. Aqueous electrolytes are easy to prepare and use. Lastly, creating a system which can work with the basic materials of nature, such as water and ionic salts, provides a great opportunity for biomedical and biochip applications in the future.

In the second chapter, brief description about conjugated polymers is given initially. Then, the properties of a polymer named poly(3-hexyl)thiophene (P3HT), which is studied in this project is described. In addition, general types of electrolytes are explained. Finally, organic thin film transistor structures are shown and electrical double layer formation is explained.

In the third chapter, fabrication and development of our electrolyte-gated organic thin film structure is explained.

In the forth chapter, we investigate the behavior of the transistor. Transistor results at the development stages are shown. Comparisons to different types of OFET are studied and we discuss the consistency of results with literature in order to realize an OFET which is sufficient enough to drive basic digital circuits. At the end, we present the result of an inverter to show the capability of the fabricated OFET.

In the last chapter, strengths of the system and important drawbacks are discussed. Possible future work is given for the thesis.

2. THEORY

2.1. Conjugated Polymers and Their Properties

The main element in many polymers is carbon atom, C. The carbon atom can form single, double and triple bonds. In its excited state ($1s^2 2s^1 2px^1 2py^1\ 2pz^1$), the 2*s* and one, two or three of the 2*p* orbitals can be combined to form two *sp*, three sp^2 or four sp^3 hybridized orbitals, respectively. In Figure 2.1 an example formation of ethane (C_2H_6) is shown. Carbon atoms are sp^3 hybridized and each C atom binds to other four adjacent atoms by sigma (σ) bond [2].

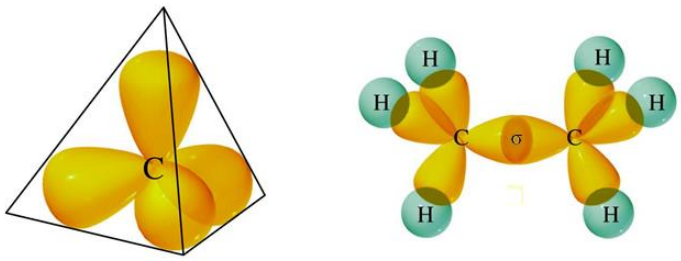

a) sp^3 hybridization b) σ bonding

Figure 2.1. Example of sp3 hybridization and σ bonding [14]

The wavefunction of the σ-electrons are formed by the large overlap between the sp^3 hybrid atomic orbitals, which causes wide σ-bands, but also high bandgap between the σ-band and the σ*-band. The high bandgap makes conventional σ-bonded polymers electrical insulators.

However, there exists another class of polymers with different properties which are called conjugated polymers. In conjugated polymers, unlike conventional structures formed entirely by σ bonds, each C atom forms three σ bonds with other atoms in the sp^2 hybridized state. The remaining pz orbital of carbon atoms overlap with each other to form delocalized π-orbitals forming π-bands (Figure 2.2) [14]. Conjugated polymers with equal bond lengths have half-filled band like metals because there is only one electron per pz orbital and there is the same numbers of π-orbitals as there are pz orbitals involved.

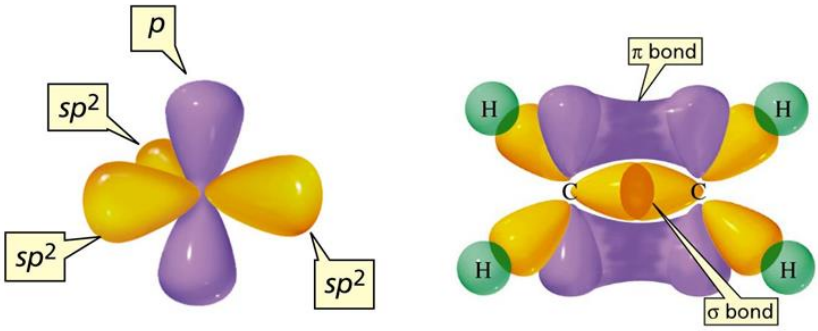

a) sp^2 hybridization b) bond forming for sp^2 orbitals

Figure 2.2. Example of sp^2 hybridization and π-bonding [14]

The electrons in these π orbitals are less localized because they are not associated with any specific atom or bond. The number of π and π* orbitals is proportional to the number of C atoms in the conjugated structure. Thus, there is a splitting of the energy levels as the number of carbons is doubled. For very long conjugated chain structures, the energies can then be described as continuous bands rather than discrete levels. The width of the band is formed according to the coupling between the atomic orbitals. Therefore, a filled valence band and an empty conduction band occur. The top of the valence band is named the highest occupied molecular orbital (HOMO), and the bottom of the conduction band is named the lowest unoccupied molecular orbital (LUMO). The energy bandgap (Eg) is defined as energy difference between these two states. It is determined from optical measurements and it is within the semiconductor range of 1 to 4 eV. In other word, pure conjugated polymers are semiconductors [2].

2.1.1. Doping in Conjugated Polymers

Doping is a common way to increase the conductivity of the conjugated polymers. It can be achieved chemically by using a redox molecule or electrochemically by charge transfer with an electrode. Examples of electrochemical doping of π-polymer as p-type and n-type is shown by the following formulas [15].

$$(\pi - polymer)_n + [Li^+(BF_4^-)]_{soln} \rightarrow [(\pi - polymer)^{+y}(BF_4^-)_y]_n + Li_{electrode} \quad (1)$$

$$(\pi - polymer)_n + Li_{electrode} \rightarrow [(Li^+)_y(\pi - polymer)^{-y}]_n + [Li^+(BF_4^-)]_{soln} \quad (2)$$

Electrochemical doping is a reversible process [16,17]. As mentioned above doping can also occur without electrochemical charge injection at a metal-semiconducting polymer interface. Polymer interface can be oxidized by hole injection into HOMO or reduced by injecting electrons into empty bands. The induced charge carriers increases the electrical conductivity but high conductivity is maintained as long as the carriers are remain injected. However, in electrochemical doping, the doping level is permanent until carriers are intentionally removed by undoping. Usage of electrochemical doping in the mechanism of transconductance in electrolyte-gated polymer FETs is discussed in more detail at the following chapters. It is shown that the carrier density can be controlled through reversible electrochemical doping [18].

2.1.2. Electrical Conduction

Conduction in conjugated structures is usually related to the mobility and the density of charge carriers. In conjugated polymers, the charge carriers are transported through hopping between localized states in the band gap. Hopping between energy states needs energy. Because of this, the hopping conductivity increases with temperature. It is worthy to mention that charges are transported via interchain hops between π-orbitals of adjacent chains. However, in an organic semiconductor film, the carriers requires to travel over a distance that by far exceeds the length of individual conjugated molecules. The charge transport in polymers is for this reason essentially determined by how the carriers move between adjacent molecules. Due to disorder and weak van der Waals intermolecular interactions, the charge carriers in conjugated polymers are usually localized to a finite number of neighboring molecules. Hence, the charge transport in organic semiconductors is limited by trapping in localized states. As said earlier, the conductivity can be increased with temperature because in-plane π -π distance reduces. However, in some cases reduction of mobility occurs due to pronounced decrease of the intergrain transport [19]. Another solution for increasing mobility is increasing carrier density. It has been shown that carrier mobility in polymer semiconductors can increase by increasing carrier density because higher carrier concentrations fills disorder-induced traps to a greater extend [20]. This situation increases the average mobility of the remaining carriers due to fewer and shallower traps [21].

2.1.3. Poly(3-hexylthiophene) (P3HT)

Polythiophene and its derivative, the poly(3-hexylthiophene) (P3HT) is one of the most examined conjugated polymer because of its good solubility and processability [2]. In this thesis, we have studied P3HT, so a brief information about this polymer is useful.

In P3HT the 3-hexyl substituent in a thiophene ring can be incorporated into a polymer chain with two different regio-regularities; head to tail (HT) and head to head (HH). A regio-random P3HT consists of both HH and HT 3-hexylthiophene in a random pattern. However, a regio-regular P3HT has only one kind of 3-hexylthiophene [22]. In organic electronics, rr-P3HT has great potentials as polymer semiconductors because it has strong tendency to self assemble into crystallites with ordered structures upon casting into thin films. As a result, it can achieve carrier mobilities in the order of 0.1 $cm^2 V^{-1}s^{-1}$[23].

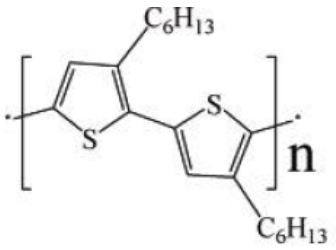

Figure 2.3. Regio-regular P3HT in head to tail order [1]

The rr-P3HT has highly anisotropic transport within the crystallites. The P3HT polymer chains can be ordered in two different orientations, parallel and normal to the substrate, according to the processing conditions and regio-regularity of the polymer. When π-stacking direction is parallel to the substrate, this implies fast and efficient interchain transport of carriers in two dimensional polymer chains. The mobility gets higher in magnitude [23]. Molecular Weight is also an important factor for the charge transport of the rr-P3HT. High molecular weight films have higher mobility [24,25]. A drawback with P3HT is that it is susceptible to oxidation [26].

2.2. Electrolytes

Electrolyte is a type of a chemical compound where salts dissociate into ions in a solvent. Due to the existence of free ions, they are electrically conductive. They are usually found in liquid phase, but molten, gelled and solid electrolytes also exist. Concentration of the salt can change ionic conductivity drastically. Depending on the solute dissociation which forms free ions, electrolytes can be put into two classes; strong and weak electrolytes. Strong electrolytes can almost be completely ionized but weak electrolytes can only achieve partial ionization. Additionally, the solvent type is important for electrochemical applications, for instance each solvent has a specific potential window to avoid decomposition [27]. The ionic conductivity of solid electrolytes is generally several orders of magnitude lower than the ionic conductivity of liquid electrolytes since it is limited by both low mobility and low concentration of ions.

2.2.1. **Types of Electrolytes**

2.2.1.1. Electrolyte Solutions. Electrolyte solutions are the most common type of electrolytes. They simply consist of a salt which is dissolved in a liquid medium. In this solution, the ions are surrounded by solvent molecules. One of the most common solvent is water. Solutions that are prepared with water is usually called aqueous solutions. Other polar non-aqueous solvents also exists; for example alcohols, ammonia etc. Even pure water is actually itself an electrolyte but a very weak one. A tiny fraction of the water molecules dissociates into hydrogen ions (OH–) and hydroxide ions (H+). Pure water has concentration of ions about 0.1 μM at room temperature, that gives a conductivity about 5.5×10^{-8} S cm^{-1}. At 77 mM NaCl solution conductivity can be increased up to the levels of 10^{-4} S cm^{-1} [28].

2.2.1.2. Ionic Liquids. They are salts in liquid state. They have relatively large anions and cations. At least one of them is generally organic and has a delocalized charge. They can have various physical and chemical properties because of the wide variety selection of anions and cations.

2.2.1.3. Ion gels. It is very difficult to use liquid electrolytes in a solid-state device. One possible solution is to immobilize the ionic liquid by blending it with a suitable polymer or polyelectrolyte which creates a gel structure for solid-state applications [29] .

2.2.1.4. Polyelectrolytes. Polyelectrolytes are polymers which possess ionized units [30]. These units dissociate when the polymer is put in a polar solvent, such as water, that results in a charged polymer chain and opposite charged counterions [31]. A dissociated polyelectrolyte in the solid state consists of mobile counterions and opposite charged polymer chains which are immobile because of their large size. Thus, solid polyelectrolytes usually transport ions of only one polarity, so they may be referred to as *n*- or *p*-type, similar to *n*- and *p*-doped semiconductors.

2.2.1.5. Polymer Electrolytes. Polymer electrolytes consist of a salt dispersed in a neutral polymer matrix, so polymer is not an electrolyte by itself [32]. The salt is dissociated into ions screened by the polymer matrix. The most common polymer electrolytes is poly(ethylen oxide) (PEO) which has repeating units of ether groups (-CH2CH2O-)n and is also known as poly(ethylene glycol) (PEG) [2].

2.2.2. Poly(ethylene glycol) (PEG)

Poly(ethy1ene-glycol) (PEG) or poly(propy1ene-glycol) (PPG) refers to polymer of ethylene oxide. PEG solutions become quite popular because of non-toxic and good heat transfer properties, compatibility with other materials and low cost. PEG with low molecular weight could exhibit high ionic conductivity when complexed with alkali metal [32]. PEG is a water soluble material, so it increases the hydrophilicity of the compound [33].

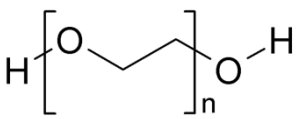

Figure 2.4. Poly(ethy1ene-glycol) (PEG)

The usage PEG is not restricted to the electrolyte solutions. There are examples where it is used in semiconductor polymer structures to increase the electrical conductivity [34]. In addition, PEG can change the hydrophobic nature of the semiconductor polymer because of its hydrophilic behaviour.

In the following chapter, we study the effect of functionalizing P3HT with PEG, which forms P3HT-co-P3PEGT polymer. We show that in aqueous solutions P3HT-co-P3PEGT polymer gives much better electrical characteristics than P3HT polymer.

2.3. Organic Thin Film Transistors

Organic transistors are metal-insulator-semiconductor (MIS) field-effect transistors (FETs) in which the semiconductor is a conjugated polymer. A thin sheet of mobile electronic charges is created at the interface of the semiconductor and dielectric when a potential difference is applied between the gate and the semiconductor. This layer of charges balances the accumulated charge located on the gate electrode. The electric current flowing through the transistor between the source and the drain contact can be controlled over a wide range by adjusting the gate voltage. Because of mobile charge induced by unintentional doping, current can flow both in the accumulation layer and the bulk of the polymer [35].

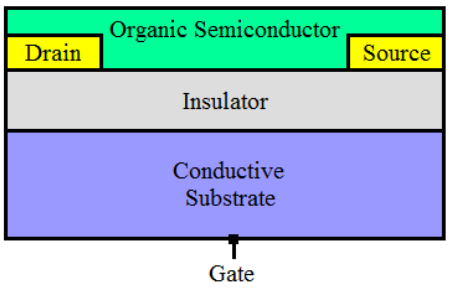

Figure 2.5. Typical MIS OFET

Organic thin film transistors can be manufactured at room temperature. In addition, it can be produced on flexible polymeric substrates which opens the possibility of creating a new range of products, such as foldable, bendable or rollable displays.

Organic semiconductors differentiates greatly depending on the choice of material, its chemical purity, and the microstructure of the solid. Semiconducting polymers that arrange in amorphous films when prepared from solution usually have room-temperature mobilities in the range of 10^{-6} to 10^{-3} cm^2/Vs [36].

2.3.1. Structures of Thin Film Transistors

There are four types of the basic structures of thin-film transistors, as shown in Figure 2.6. Structures can be divided as top-gate and bottom-gate structures according to the position of the gate electrode. Top-gate structure has gate electrode on the semiconductor layer, other one has it under the semiconductor layer. Second categorization depends on the position of the source and drain. When the source-drain electrodes are located at the opposite side of the gate, it is called a staggered structure. The other is named planar structure when all electrodes are located at the same side of the semiconductor layer.

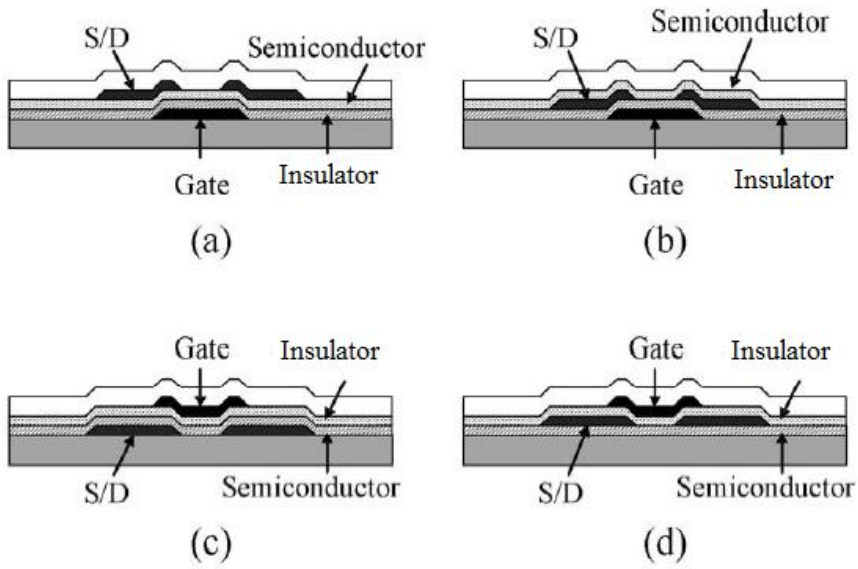

Figure 2.6. OFET structures (a) Staggered, Bottom-Gate, (b) Planar, Bottom-Gate (c) Staggered, Top-Gate, (d) Planar, Top-Gate [36]

It is important to understand which structure forms the best FET. FET characteristics depend on the materials that are used, for example top-gated structures are more suitable for electrolyte-gated transistors. However, it has been found that thin film

transistors with staggered structure have more current flow, bigger field-effect mobility, and lower contact resistance than the planar structure [37]. The source electrode of the staggered structure has better ability to supply current because it can use whole upper surface of the source at the case of saturation.

2.3.2. Electrical Double Layer Capacitance (EDLC)

In a metal-electrolyte-semiconductor system, electric potential difference between the metal electrode and the electrolyte results in the formation of a charged interface. The induced electronic charges in the metal electrode reside on the outermost surface of the electrode, while an excess of compensating and oppositely charged ions are located in electrolyte, close to the metal interface. Thus, a second layer is formed by opposite charged ions at the semiconductor-electrolyte interface. As we can see from Figure 2.7, V_G applied to the gate electrode produces a negative surface charge on the metal that attracts mobile cations in the electrolyte at the gate-electrolyte interface. Negative ions are pushed from the gate and a layer of anionic charge is created at the opposite electrolyte-semiconductor interface. The resulting induced charges at the surface of the semiconductor provide a conductive channel between drain and source electrodes [13]. This system of two parallel layers of positive and negative charges is called an electric double layer (EDL) and the created capacitance is called electrical double layer capacitance (EDLC).

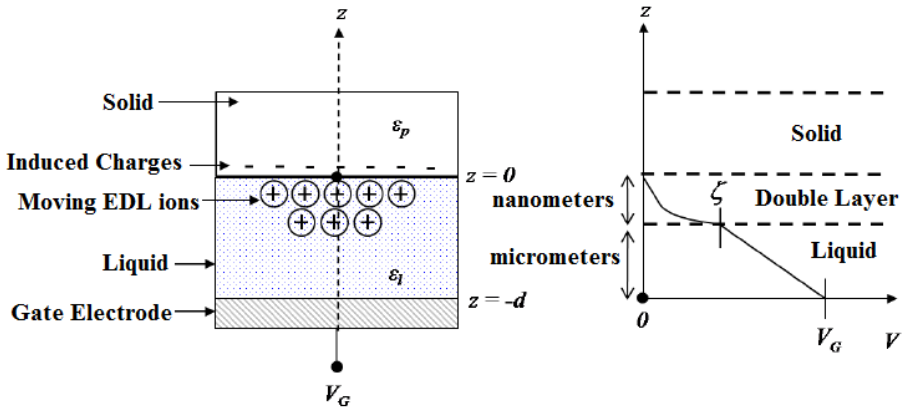

Figure 2.7. Formation of EDL in Metal-Electrolyte-Semiconductor System

This formation removes the need of insulator layer between gate and the semiconductor by creating same induction effect of the MIS. In addition, the magnitude of

field effect created by thin layer capacitance at the semiconductor surface cannot be achieved practically by solid thin films of insulators. It has been shown that even at high frequencies capacitance of the electrolyte gate is more than two orders of magnitude larger than that of the 100-nm-thick SiO_2 gate dielectric [38]. In addition, maximum carrier density is also considerably larger than SiO_2 gate dielectric. Thus, EDLC provides a great opportunity for low voltage applications because the achieved channel induction in SiO_2 dielectric structure with 60 V can easily be achieved by 1 V gate voltage in EDLC systems [39].

2.3.3. Thin Film Transistors for Sensor Applications

In the MOSFET, the threshold voltage depends on the metal and the semiconductor. The electrolyte-gated OFET situation is different than this. In this case, the gate is replaced by a reference electrode, so the threshold voltage is also sensitive to the interfacial potential at the electrolyte–semiconductor interface. Thus, any change in this interfacial potential, such as the presence of charged molecules would result in a shift of the conductance of the semiconductor. Electrolyte gated organic thin film transistors can be grouped as: organic electrochemical transistors (OECT) which are based on electrically conducting polymer (ECP) and organic field-effect transistor (OFET), composed of an organic semiconductor (OSC) [40].

2.3.3.1. Organic Electrochemical Transistors (OECT)s. The operating principle of OECTs depends on the doping and dedoping of the polymer, which results in modification of its conductivity. Typical electrochemical polymers are polypyrrole, polyaniline and polythiophene [41]. Typically, an OECT converts an ionic current into an electronic current. Thus, it can be used for monitoring biological phenomena. In addition, their operation at very low voltages, such as 1V is also a great advantage. This ability make OECTs suitable for biosensing in aqueous media, where low voltages are required to avoid undesired redox reactions in water or biomolecules [40]. Typical OECT structure is shown in Figure 2.8. As will be explained in the coming sections, the transistor structure of OECT is very similar to the electrolyte-gated OFET. The difference does not originate from the structure but the transistor operation. However, in electrical double layer transistors, the ions do not penetrate the polymer layer, and the operation of these devices relies on a field effect rather than on electrochemical doping-de-doping. But EDLC transistor can also

benefit from these results because most conducting polymers have been optimized for electronic conductivity, and improvements can be achieved by the optimization of permeability to ions [42].

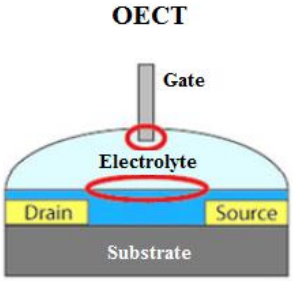

Figure 2.8. Organic Electrochemical Transistor [40]

2.3.3.2. Organic field-effect transistors (OFETs). There are four types of OFETs that are used in biomedical and sensor applications. The first one is a classical architecture with insulated gate operated in dry state (Figure 2.9a). Second one uses classical architecture for sensing applications in aqueous medium (Figure 2.9b). Third one is an ion sensitive OFET (ISOFET) where a reference electrode is used as gate electrode and the drain current is driven by the potential of the electrolyte–insulator interface (Figure 2.9c). By making the insulator sensitive to a given analytic, it is possible to detect a wide range of biomolecules [40].

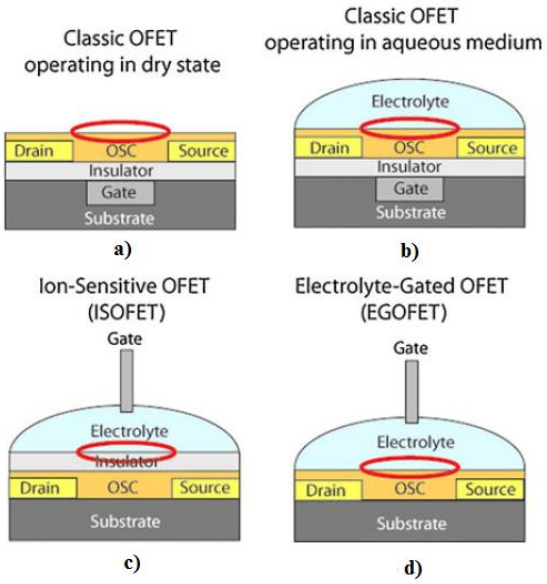

Figure 2.9. OFET structures for Chemical Sensing [40]

Fourth one is electrolyte-gated OFET (EGOFET) structure (Figure 2.9d). EGOFETs have recently gained much attention because of low voltage operation compared with OFETs gated via solid dielectrics. EGOFETs differ from OFETs, as in OECTs, the gate is separated from the semiconductor by an electrolyte forming an electrical double layer (EDL).

In electrolyte-gated OFETs, in order to use solid processable materials, polyelectrolytes or polymer electrolytes have been used extensively [43, 44, 45]. But these type of solid electrolytes have low ionic mobilities, so large gate voltage drop occurs between the gate electrode and the semiconductor-electrolyte interface. Thus, gate electrode proximity to the channel is an important parameter for solid electrolytes. This situation restricts the flexibility of gate electrode location for solid electrolyte systems.

2.3.3.3. OFETs operating in Aqueous Media. One issue with EGOFETs is that electrochemical switching and field-effect modulation of the organic channel often coexist because common ionic salts can penetrate into the organic semiconductor. This situation disrupts the ideal EDL formation and results in transistors that are typically slow and that exhibit a great degree of hysteresis. Using solid polyelectrolytes is not practical for simple biomedical and sensor applications. A novel system is proposed using DI Water as an electrolyte that operates entirely in the field effect region [46]. P3HT is used as the organic semiconductor in this system (Figure 2.10). It has been shown that EDLC formation saturates below 10 Hz which indicates that dense electric double layers have been created at both sides.

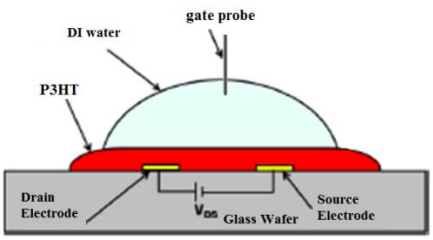

Figure 2.10. Water Gated OFET

This device structure is simple and easy to produce. It could reveal a very helpful tool for rapid testing of new organic semiconductor compounds.

Organic semiconductors are known to be electrochemically active. It is usually debated whether the increase in conductivity in electrolyte-gated organic transistors is due to the field effect or electrochemistry. The first effect is entirely driven by the accumulation of ions at the semiconductor-electrolyte interface but the latter requires ions to pass that interface and to migrate into the semiconductor bulk.

Although, hysteresis free behavior of DI Water, in order utilize the OFET structure in chemical sensing water should host ions to be detected. It may be tolerable to use diluted aqueous solutions with this structure for sensing applications because of several reasons. First of all, higher ionic concentration leads to faster polarization time due to faster electrical double layer formation ,so this increases the transconductance of the OFET which is also beneficial for circuit applications [47]. Faster polarization can also be achieved by NaCl [48]. Nevertheless, the rather high hysteresis compared to P3HT signifies that ion penetration still occurs.

Moreover, semiconductor carrier mobility of electrochemical doping at low doping levels was lower than that of field-effect doping by two orders of magnitudes , so electrochemical doping can be tolerable for dilute solutions. However, electrochemical doping steeply increases according to the doping level and becomes comparable or higher values than that of field-effect doping [49]. In addition, doping is highly reversible [50]. Ideal region of operation can be found with OFET experiments at different soluble concentrations.

2.3.4. Transistor Characteristics

As mentioned before, the conductivity of the induced channel is enhanced upon increasing the gate voltage because OFETs normally work in the accumulation mode. The general behavior in OFET characteristics can be described by conventional semiconductor theory. The general current-voltage formula can be described as:

$$I_{D,linear} = (W/L)\mu_{linear}C_i(V_G - V_T - \left(\frac{V_D}{2}\right))V_D \quad (3)$$

$$I_{D,saturation} = (W/2L)\mu_{saturation}C_i(V_G - V_T)^2 \quad (4)$$

Where L is used for length between drain-source electrodes , W is used for the transistor channel width, μ is used for mobility of the semiconductor polymer which changes with operation region and C_i is used for gate dielectric capacitance per unit area.

In order to evaluate the performance characteristic of an OFET, some parameters bear specific importance. The common reported parameters are on/off current ratio, transconductance (g_m), mobility, threshold voltage and sub-threshold slope. On/off current ratio can be seen from I_D-V_{DS} output graph (Figure 2.11, left). Threshold voltage and transconductance can be seen from I_D-V_{GS} transfer graph. In our discussions for circuit application, on/off current ratio and transconductance parameters are especially used.

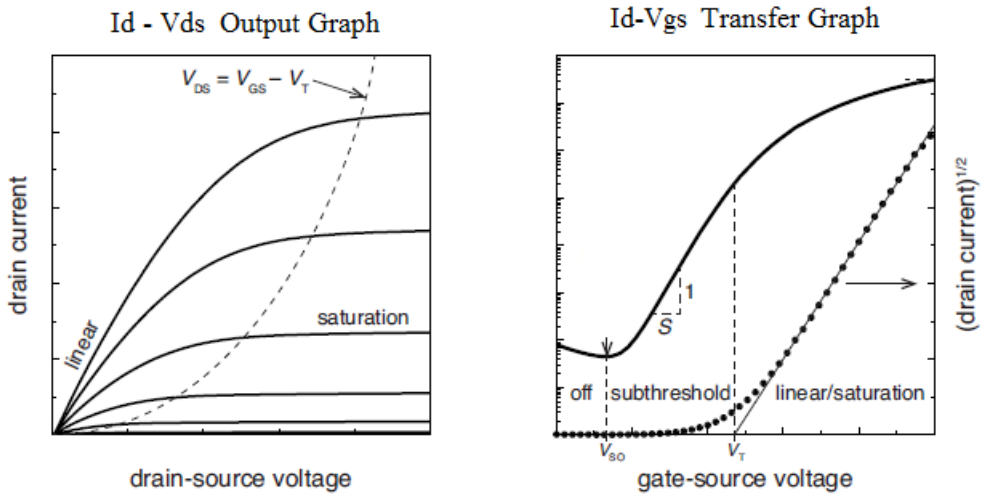

Figure 2.11. Illustration of OFET output characteristics,
(left) I_D-V_{DS} output graph, (right) I_D-V_{GS} transfer graph [1]

In OFET g_m can be defined as the change of I_{DS} with V_{GS} for a constant V_{DS}. It is preferable to take two transconductance parameters as $g_{m,lin}$ and $g_{m,sat}$ to see the quadratic behavior at different operation regions.

$$g_m = \frac{\partial I_D}{\partial V_{GS}} \qquad \text{for constant } V_{DS} \tag{5}$$

From the current-voltage formula, the linear and saturation mobilities can be determined:

$$\mu_{linear} = \left(\frac{\partial I_{D,linear}}{\partial V_G}\right)\left(\frac{L}{WC_iV_D}\right) \tag{6}$$

$$\mu_{saturation} = \left(\frac{\partial (I_{D,saturation})^{1/2}}{\partial V_G}\right)\left(\frac{2L}{WC_i}\right)^{1/2} \quad (7)$$

The on/off current ratio ($I_{on/off}$) can be found from:

$$\frac{I_{on}}{I_{off}} = \frac{I_{D,sat}\,(V_{Gmax})}{I_{D,sat}\,(V_{G=0})} \quad (8)$$

2.3.5. PMOS Inverter

Inverter is the most basic logic gate for digital circuits. The output characteristic of the inverter can represent the reliability of the OFET structure and the interaction capability with other digital systems. As mentioned earlier, in this project P3HT is used as the semiconductor polymer and P3HT gives induction channel characteristic of a PMOS transistor. Hence, PMOS inverter is implemented from our organic thin film transistors. There are two types of PMOS inverter structures.

In resistive load inverter, lower PMOS is connected to the low bias of the circuit. Thus, it is always open and acts as a resistor. In this structure, pull-down speed is high but the gain of the transistor is small due to low output resistance [51]. In resistive load inverters, the ideal response is realized when the load resistance is twice the channel resistance of the transistor in its on state. Thus, in order to get better performance, the driver transistor should be made 2 times larger in saturated load inverters [52].

In depleted load inverter, load transistor is connected to the output. This configuration provides high gain to the inverter because resistance becomes very high when driver PMOS is conducting [8]. Thus, load transistor behaves like a diode. This is why depleted load inverter is also called diode loaded inverter. In depleted load configuration, load transistor can be taken r times larger in order to increase the pull-down speed of the transistor.

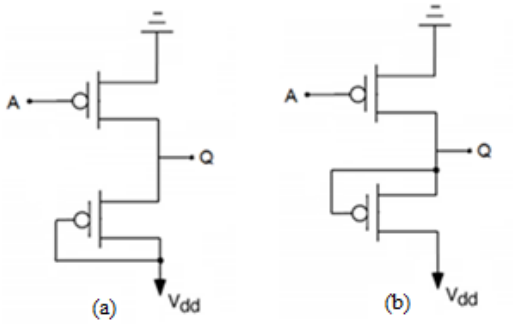

Figure 2.12. PMOS inverter (a) Resistive Load Inverter, (b) Depletion Loaded Inverter

In our measurements, inversion rate and gain are significant parameters for characterization. The inverter needs to have a voltage gain larger than unity in order to drive other subsequent gates. Figure 2.13 shows typical inverter parameters [1].

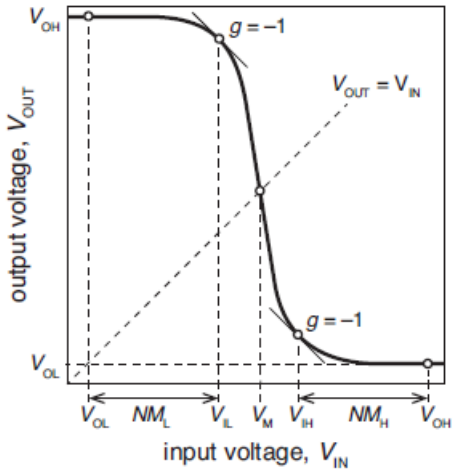

Figure 2.13. Transfer Characteristics of the Inverter [1]

3. FABRICATION

3.1. Fabrication Equipment

Photolithography is an important process for MEMS fabrication processes. In our project, photolithography is extensively used to form electrodes which are used in the OFET structure. UV exposure lamp is a crucial device for photolithography. As can be seen from Figure 3.1, it consists of UV lamp, power source and a vacuum pump. The lamp can give UV light in a uniform manner with 20 mW/cm^2 intensity. Wavelength of the light is 365nm.

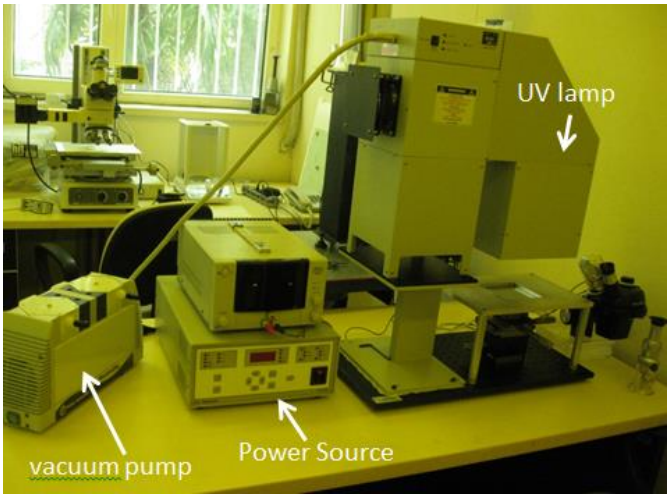

Figure 3.1. UV Exposure Device

In Figure 3.2, there are two heating tables which are used for the annealing treatments. Oxygen plasma cleaner is usually used for cleaning and etching P3HT on the glass wafer.

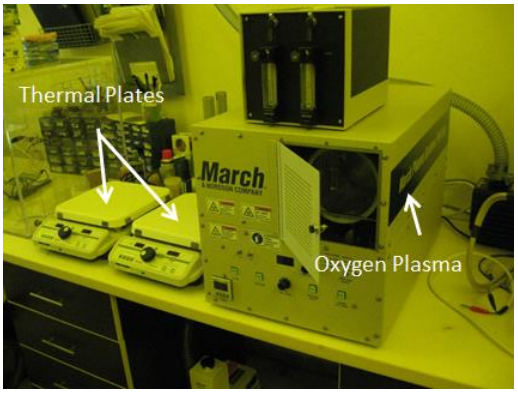

Figure 3.2. Oxygen Plasma and Heating Tables

In Figure 3.3, spin-coater is shown. This equipment is used for coating photoresist and polymer solutions to the surface of glass wafer.

Figure 3.3. Spin Coater

In this project, Keithley SCS 4200 semiconductor parameter analyzer is used as the measurement terminal (Figure 3.4). The probe station is used to form contacts to the electrodes on the glass wafer.

Figure 3.4. Keitley SCS 4200 and Probe Station

3.2. Basic Electrode System for Test Application

In order verify the transistor characteristic of the DI Water gated P3HT OFET transistor, we have designed a simple test structure. The aim was to form a structure as in Figure 3.5.

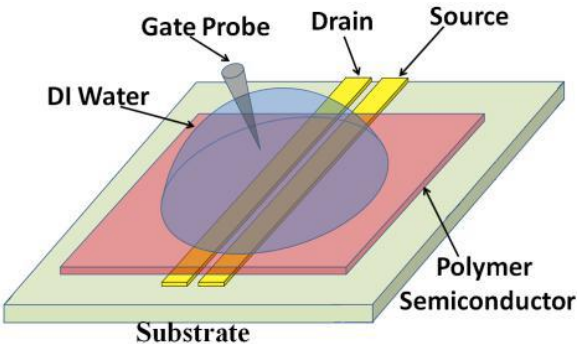

Figure 3.5. Water Gated simple OFET structure

In this design drain and source electrodes are coated with P3HT. There is a drop of DI water put on the P3HT and the gate potential is supplied to the system by the measurement probe of the probe station.

Forming source and drain electrodes is the first step of this fabrication. We use Chrome-Gold coated 4-inch wafer for this. The thickness of the glass wafer is 500µm. The thickness of chrome and gold films are 5 nm and 50 nm, respectively. We use PR1828 photoresist for lithography process which is a positive photoresist. The photoresist is coated on the glass wafer by spin-coater at 2000 rpm. The thickness of the resist layer is about 5µm. Then, resist is baked at 90 $^{\circ}$C for 1 minute. After the soft bake, wafer is exposed to UV light for 1.5 minutes. The mask used during the process is given in Figure 3.6. Figure 3.7 is used to form gate electrode to create a staggered-top gate test structure.

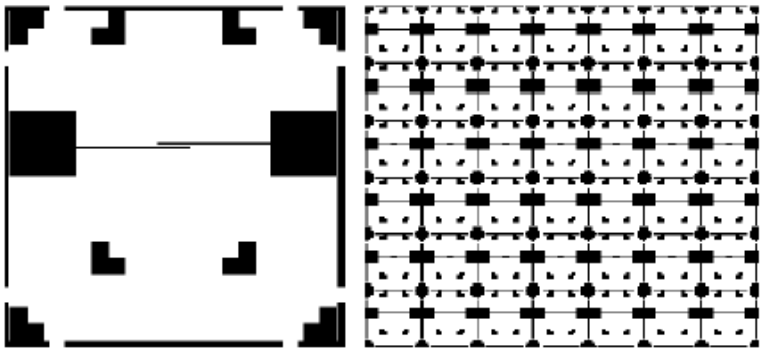

Figure 3.6. Mask of source-drain electrodes and its pattern over the wafer

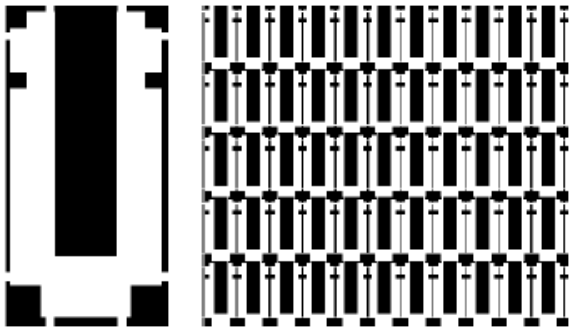

Figure 3.7. Mask of gate electrode and its pattern over the wafer

Then, photoresist is developed in MF26A developer for 1.5 minutes. After DI water rinsing and drying, wafer is put into the gold etchant. Photoresist is removed with acetone before chrome etching because there is a chemical reaction between chrome etchant and resist. Electrode forming is finished by chrome etching, photoresist layer is not needed at chrome etching because of the gold layer. Formed electrodes can be seen in Figure 3.8.

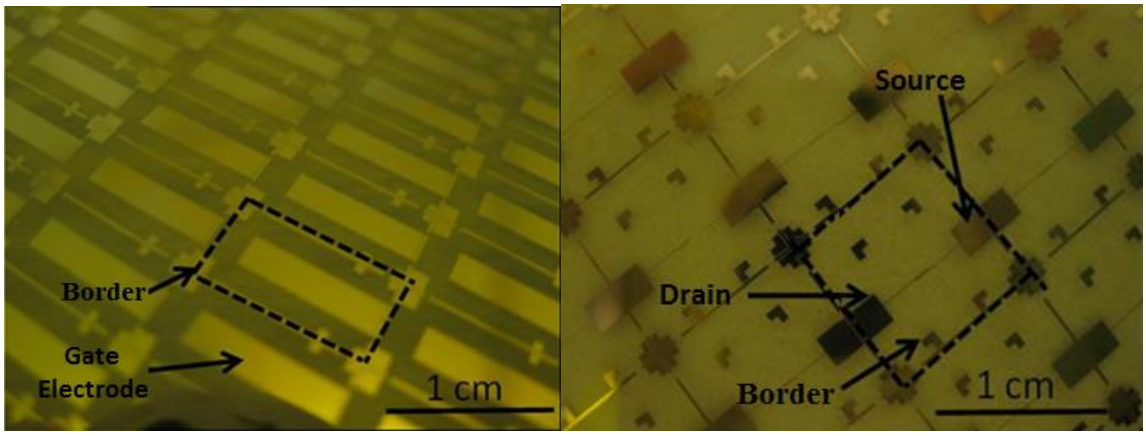

Figure 3.8. Gate Electrode Wafer (left), Drain-Source Electrode Wafer (Right)

The drain-source test platform has 1cm x 1cm area and the gate top electrode has 0.5cm x 1 cm area. Channel region has width of 1 mm (W) and length of 50µm (L). Drain and source electrodes are symmetric and their widths are 50µm. Width of gate electrode is 2mm.

Afterwards, dicing process is applied to the wafers from the borders to separate the individual transistor platforms. In the second step, regio regular P3HT from Sigma-Aldrich is prepared as a solution. Chloroform is used as solvent material because of rapid evaporation. Aldrich rr-P3HT has average molecular weight between 55000-75000. After

couple of trials and with the help of literature, 2 mg rr-P3HT per 1 mL chloroform is decided for concentration. After the preparation of the solution, it is put into the ultrasonic cleaner for 1 hour to complete dissociation of the P3HT. Then, solution of P3HT is applied to the drain-source electrode platform by drop-casting.

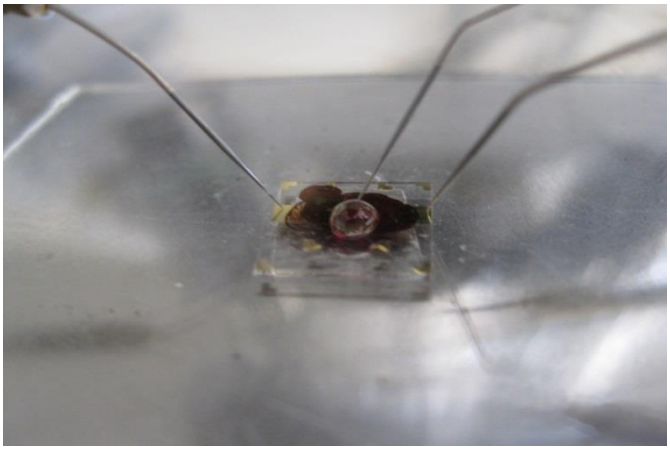

Figure 3.9. Water Gated OFET with Tungsten Probe as Gate Electrode

In Figure 3.9, it can be seen that DI water is dropped on top of dried P3HT layer. Due to the hydrophobic behavior of the P3HT water drop can stay in hemispheric shape. Gate voltage is applied by measurement probe. The output result is shown in Figure 3.10.

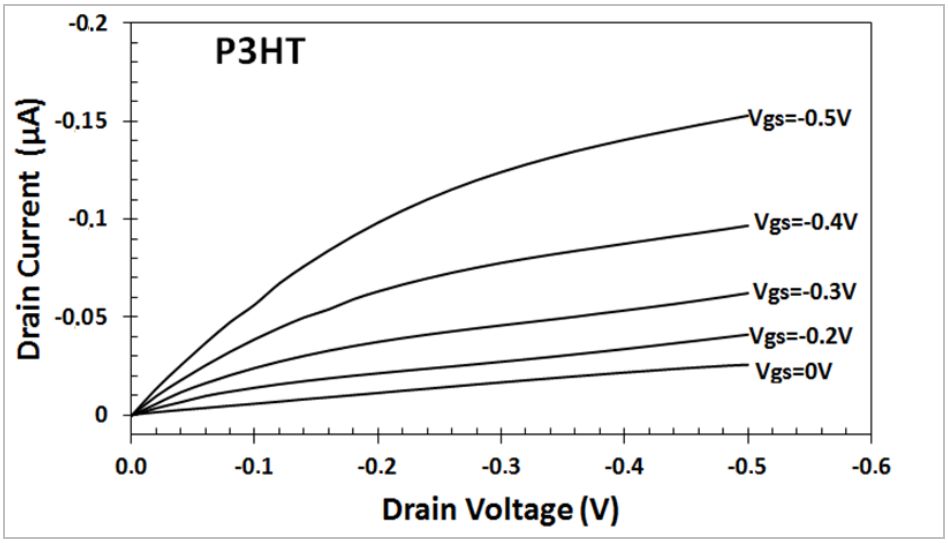

Figure 3.10. I_D-V_{DS} output graph of Water Gated OFET with Probe

Although, the I_{ON} and the on/off current ratio ($I_{ON/OFF}$) is very low, this graph proves that our water gated OFET structure is operational. In order to see the effect of staggered-top gate structure, gate electrode is put on top water as in Figure 3.11. Because

of the capillary force gate electrode can stick to the drain-source platform. One important issue of this structure is that it is hard to protect source and drain electrodes from water contact, otherwise leakage current occurs.

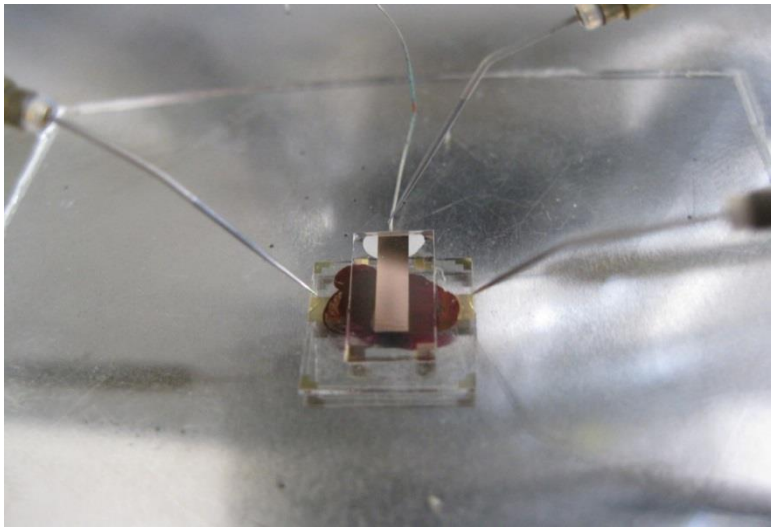

Figure 3.11. Staggered-Top Gate OFET

The output result of the top gate structure is given in Figure 3.12.

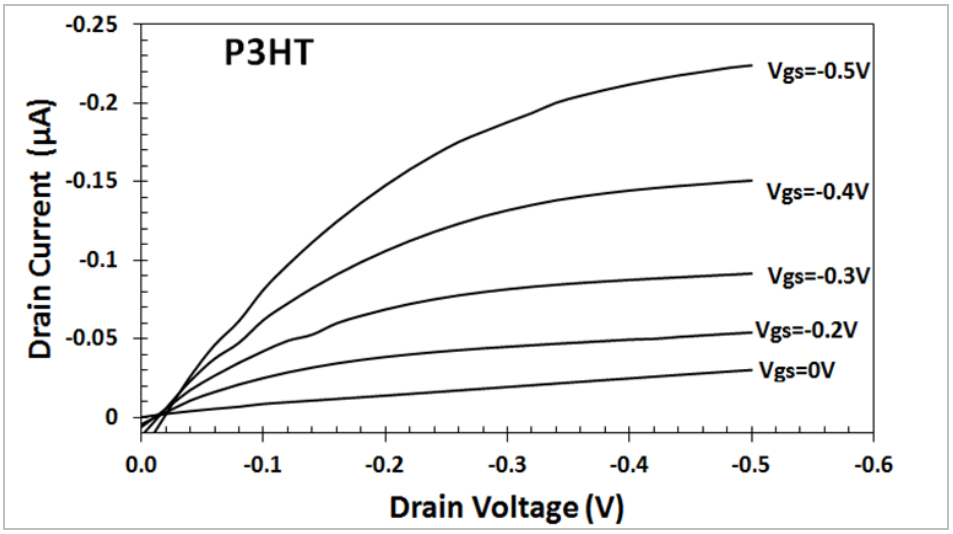

Figure 3.12. I_D-V_{DS} output graph of Staggered-Top Gate OFET

Although, there is an increase on current of the transistor, it can be expected that much larger area of the gate electrode and greater proximity to the channel region should have provided much better transistor characteristics. It should also be mentioned that gold has better work function with P3HT than tungsten probe [46]. However, results are

consistent with the theoretical behavior. Since mobility of electrolyte solutions are high [2], proximity is not crucial for liquid gated OFETs.

In the staggered-top gated test structure, one challenge is that it is difficult to position gate on top of the channel. Thus, we cannot get consistent results. Change of experimental setup is high for this kind of individual structure. As a result, the circuit operation cannot be realized with this system. The next step is to create a transistor structure that gives more consistent results to the repeated experiments.

3.3. Water Gated OFET with Planar Gate Electrode

As mentioned earlier, in order get consistent results we need to build stable electrode position, so their effects to the transistor can remain constant. In addition, study of this thesis is a subset of ongoing TÜBİTAK project that the ultimate aim is to form microfluidic channel on the water gated OFETs. Thus, water can be confined and its effect can be stabilized by the fluidic channel formation. However, it is very challenging to form the gate electrode on top of P3HT and water layer in the microfluidic channel. As a result, a novel solution is proposed that allows us to use the mobility advantage of the ionic liquids. It is forming the gate electrode on the same substrate with drain-source electrodes, so all tree electrodes are on the same plane. An illustration showing this structure is shown in Figure 3.13.

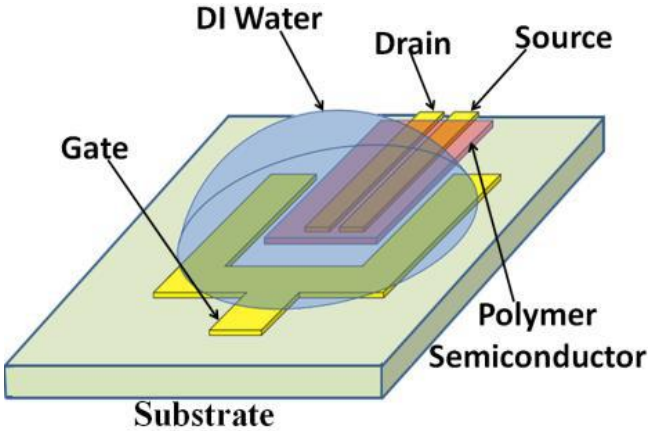

Figure 3.13. Structure of OFET with Planar Gate Electrode

As can be seen from the structure, all electrodes are formed on the substrate together. P3HT coats only the drain-source region. It does not touch the gate electrode. Thus, applied potential from gate results in electrical double layer capacitance formation at

the water-P3HT channel interface. Before implementing this structure, it has been verified with measurement probe that OFET is still operational even the probe is 5mm away from the channel region.

Figure 3.14 represents the mask drawing of the new transistor structures in L-Edit layout tool. Red color indicates the electrode layer. Green layer is used for P3HT patterning. Other layers denote microchannel structure.

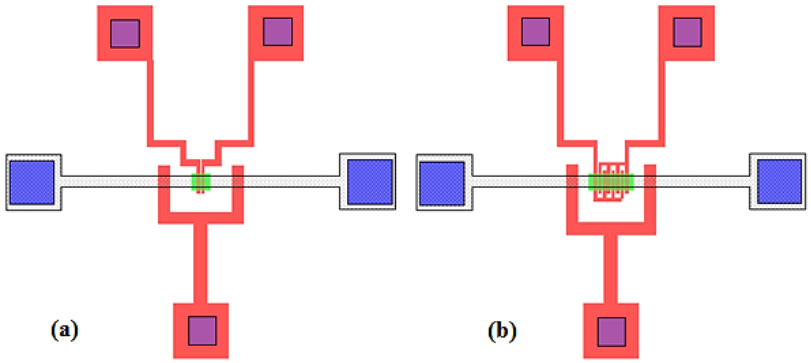

Figure 3.14. L-Edit Drawing of The OFET with Planar Gate Electrode
(a) Single D-S Model, (b) Interdigitated D-S Model

In the planar gate design, source and drain electrodes are brought as close as possible according to the resolution of the mask printer system. Hence, the distance between drain and source becomes 30 µm (L). Width of the drain-source is different for microfluidic channel system because water is confined within channel that has 200 µm width. In the test setup that uses water drops, water covers larger electrode area. Width of the channel in this case is approximately 600 µm. Gap between the source-drain legs are still 50 µm (L). The distance of gate electrode from the source-drain region is 500 µm and gate electrode has width of 200 µm.

In order to increase the performance of the transistor, an interdigitated transistor model is also designed, which can be seen in Figure 3.14b. There are four drain and source finger couples. Each has channel length of 30 µm. Width of the drain-source legs are still 50 µm. The distance of the gate electrode from the outermost drain-source legs is 300 µm. The mask set of the new design is implemented on Cr-Au coated glass wafer. The microscope images of the planar gate structure are given in Figure 3.15.

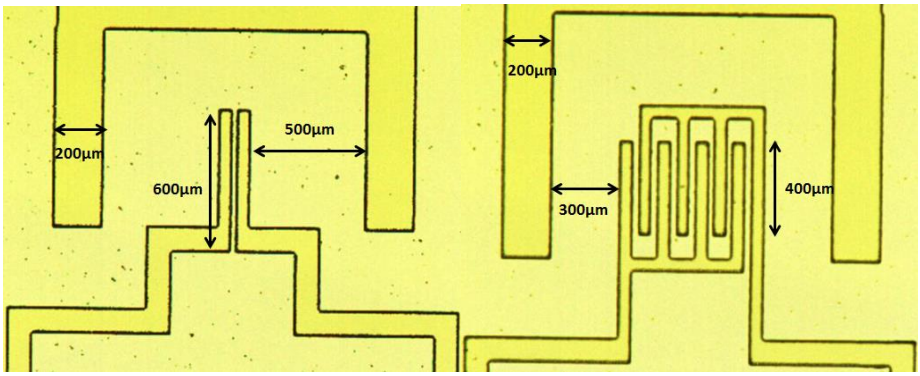

Figure 3.15. Microscope Image of Planar Gated Electrodes

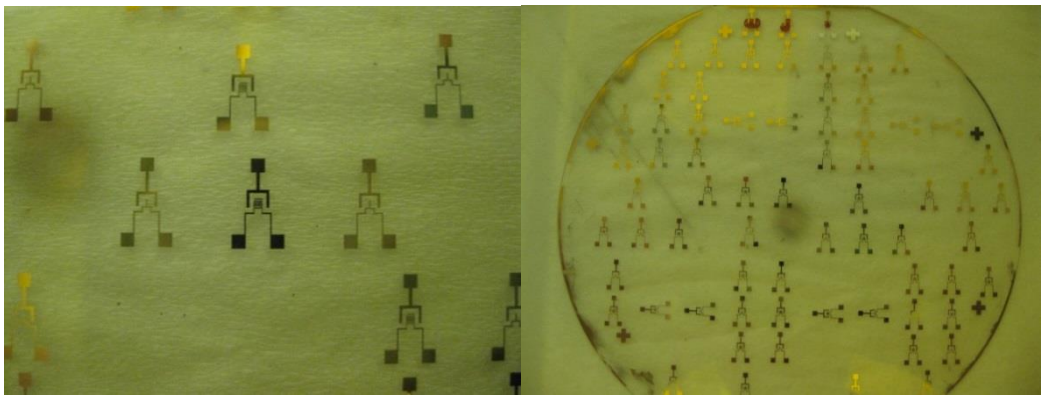

Figure 3.16. Images of the electrode wafer

The first tests of the transistors are performed by drop-casting of rr-P3HT solution, which can be seen in Figure 3.17. In order to supply potential from gate to the water electrolyte, top of the gate electrode is cleaned from P3HT by a sharp tip under microscope. Then, a drop of DI water is placed over the channel region. Results are given in the next chapter.

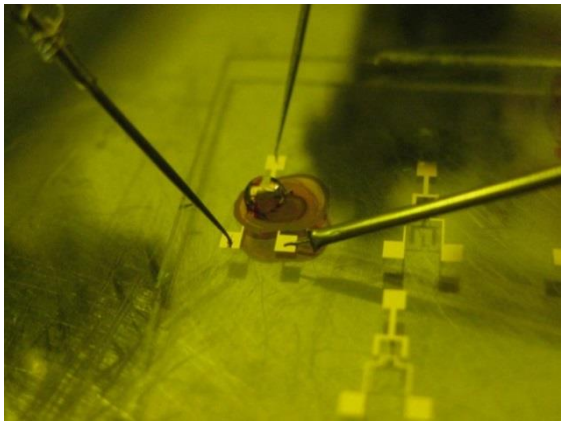

Figure 3.17. Water gated OFET with Planar Electrode Contact

3.4. Building Basic Circuit Application

The new planar gate structure of OFET electrode system provided the opportunity of building basic circuit applications, such as inverter and oscillator more easily. As a result, second mask set is designed for the circuit application of the OFET. PMOS inverters are drawn based on the lateral gate electrode structures. L-Edit layout of the designed inverters is shown in Figure 3.18.

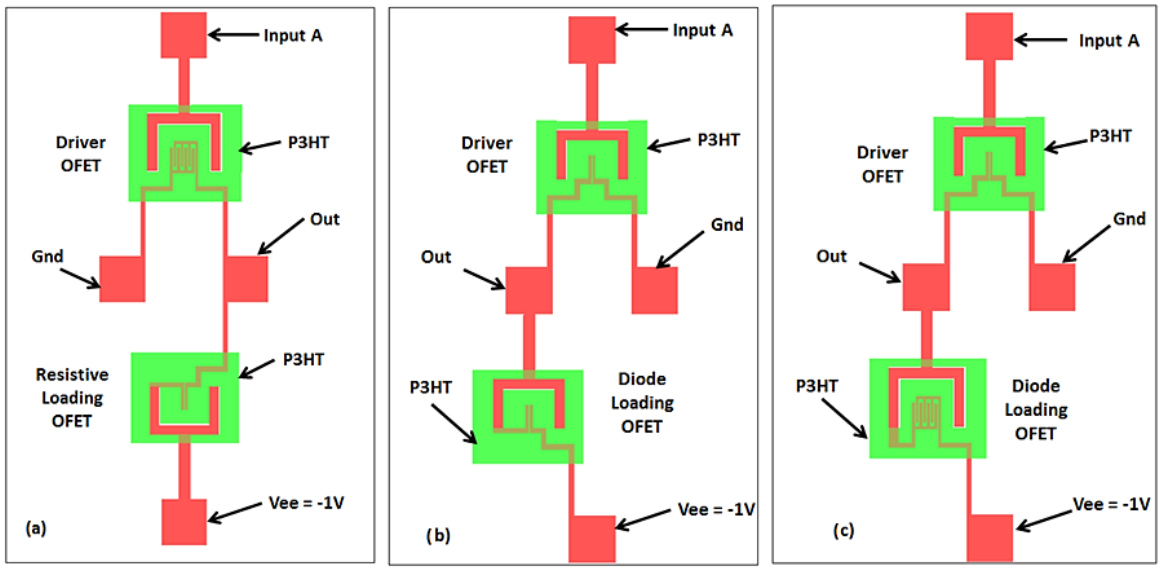

Figure 3.18. Planar Gated OFET PMOS Architectures
(a) Interdigitated-Single Resistive Loaded, (b) Single-Single Depletion Loaded,
(c) Single-Interdigitated Depletion Loaded

Three types of inverter are implemented in the new design. First one is a resistive loaded inverter (Figure 3.18a). As mentioned at the theory of PMOS transistor drain and gate of the load transistor is connected to each other. Interdigitated transistor is used for driving transistor in order to give better pull-up to the output when the input is low. Figure 3.18b and Figure 3.18c have depletion load inverter connection. Both transistors have output and the load gate connected to each other. In Figure 3.18c, load transistor is enlarged by interdigitated transistor scheme. 3-stage ring oscillators are also designed from these inverter structures as can be seen in Figure 3.19.

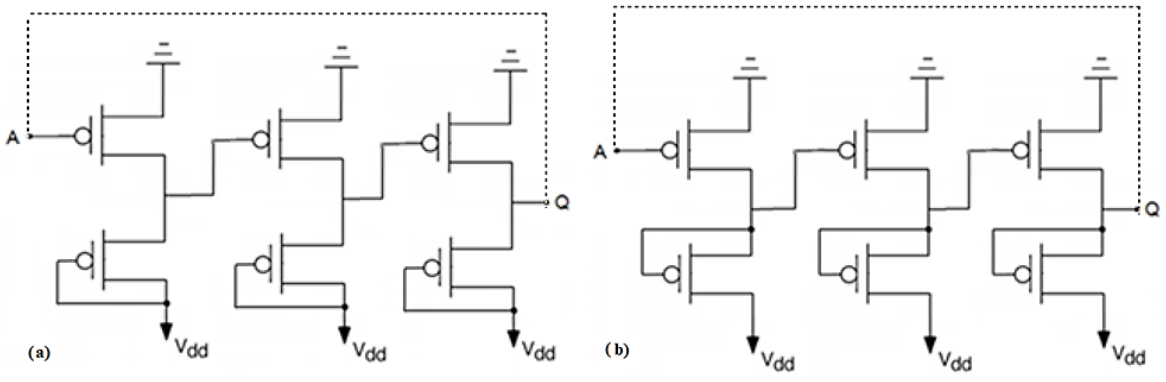

Figure 3.19. 3-stage ring oscillator schematic

(a) Design with resistive loaded inverter, (b) Design with depletion loaded inverter

According to the ring oscillator circuit schematic, when the input of the first inverter stage ‘A’ is connected to the output of the last inverter ‘Q’, the circuit starts to oscillate. However, the required condition for oscillation is that the gain of each inverter must be greater than ‘1’. Thus, our aim in this thesis is to build an inverter with high gain characteristics. In Figure 3.20, layouts of oscillator designs using three different PMOS inverter types are presented.

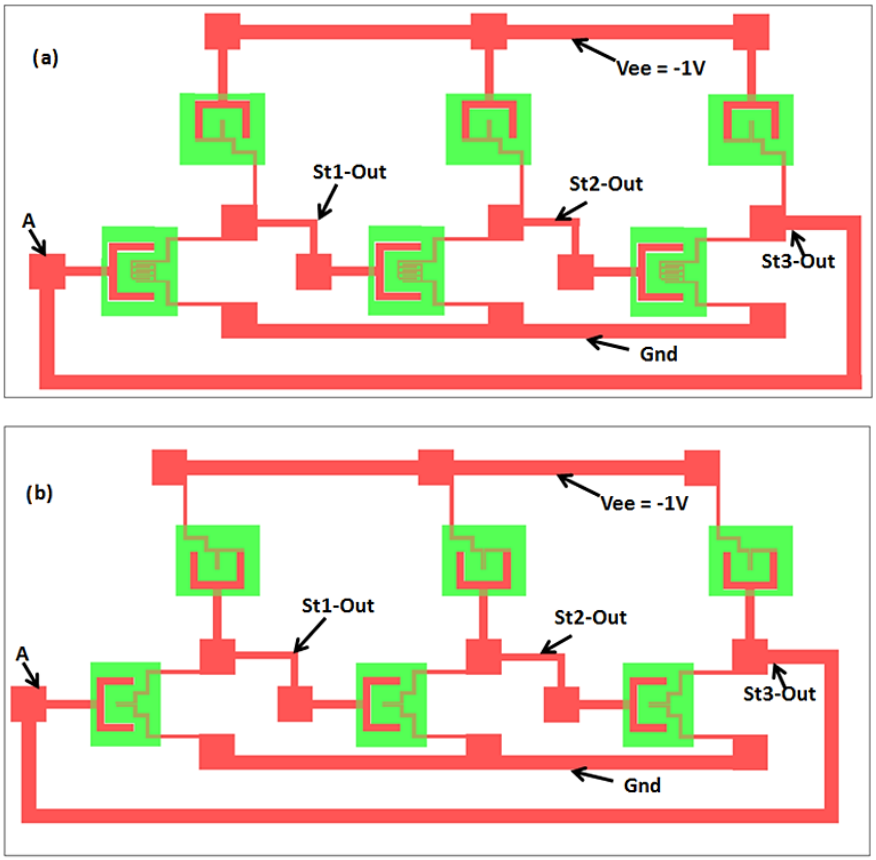

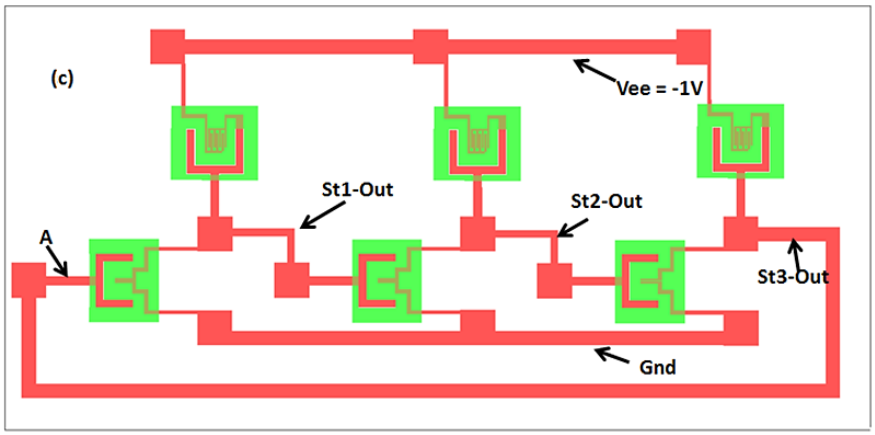

Figure 3.20. L-Edit Oscillator Layouts
(a) Resistive Loaded Layout, (b) Single-Single Depletion Loaded Layout,
(c) Single-Interdigitated Depletion Loaded Layout

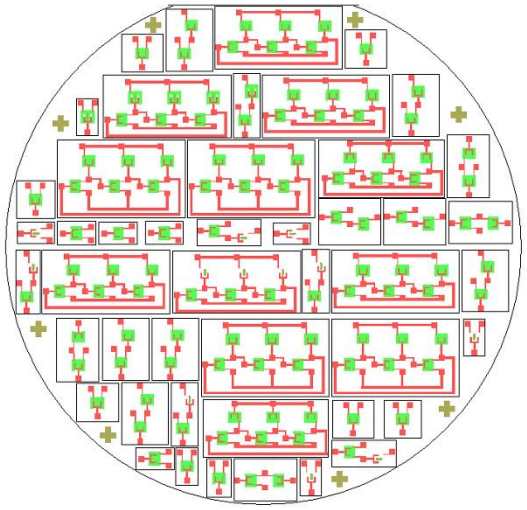

Figure.3.21. L-Edit layout of the circuit mask

The new mask set is also implemented on Cr-Au coated glass wafers. Figure 3.21 shows the fabricated electrode structure of the designs.

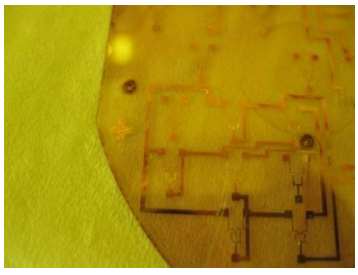

Figure 3.22. Image of the inverter and oscillator electrode platform

3.5. Test Experiment for the Synthesized Semiconductor Polymers

The new EGOFET structure has a unique structure since it uses water as gate insulator. Therefore, water has to form a good interface with P3HT. However, P3HT is hydrophobic in nature. This implies that the performance of the EGOFET can be improved if a hydrophilic semiconductor polymer is used. Functionalized poly(3-hexylthiophene) polymers can be synthesized in order to improve the interface of the polymer with the aqueous electrolytes. These efforts are shown by our collaborators, Associate Prof. Dr. Amitav Sanyal and Ph.D. student Kader Merve Turksoy at the Chemistry Department of Bogazici University. They started their work by first synthesizing regio-regular poly(3-hexylthiophene).

The synthesized regio-regular P3HT is tested in planar gated OFET structure in order to see the characteristic of the polymer. However, no meaningful result is observed. Afterwards, it is concluded that the reason of the variation between the behavior of the commercial product and the synthesized product is their chain length differences. There is a direct correlation between the chain length and the molecular weight of the polymer. It has been shown in the literature that higher molecular weight increases mobility effectively [24].

The molecular weight of the synthesized regio-regular P3HT is between 10000-30000 whereas commercial product has the molecular weight between 55000-75000. Since the synthesized polymer chains are shorter, they cannot close the large gap of 30 μm between the source and drain electrodes efficiently, resulting in almost an open circuit situation. Due to this, we build a diode structure in order to confirm the functionality of the synthesized rr-P3HT. It is possible to build a schottky diode by sandwiching the polymer film between two metal electrodes, one of which has ohmic and the other has schottky contact [53]. Hence, a diode configuration is implemented by sputtering aluminum on the rr-P3HT coated gold electrodes. Figure 3.23 shows the diode and the measurement system.

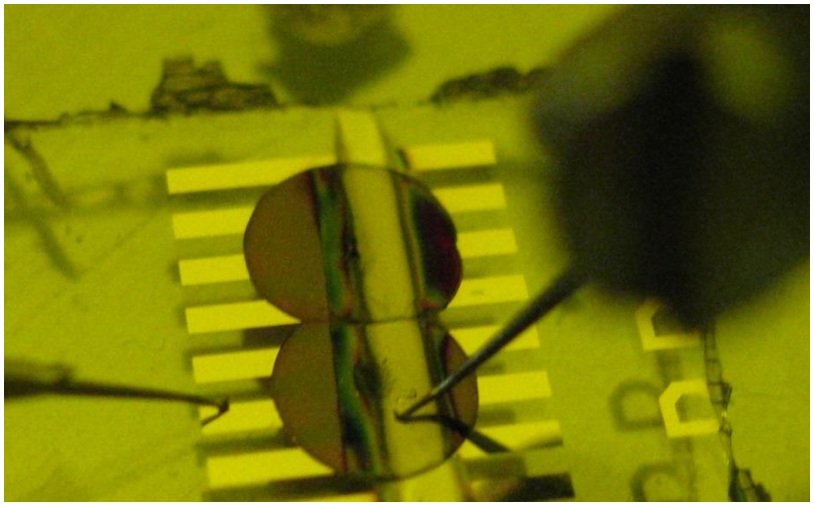

Figure 3.23. Schottky diode with rr-P3HT

According to measurement results seen in Figure 3.24, it is shown that the synthesized rr-P3HT is functional and works as a semiconductor and it requires a new electrode structure with very small gap forming a shorter channel length.

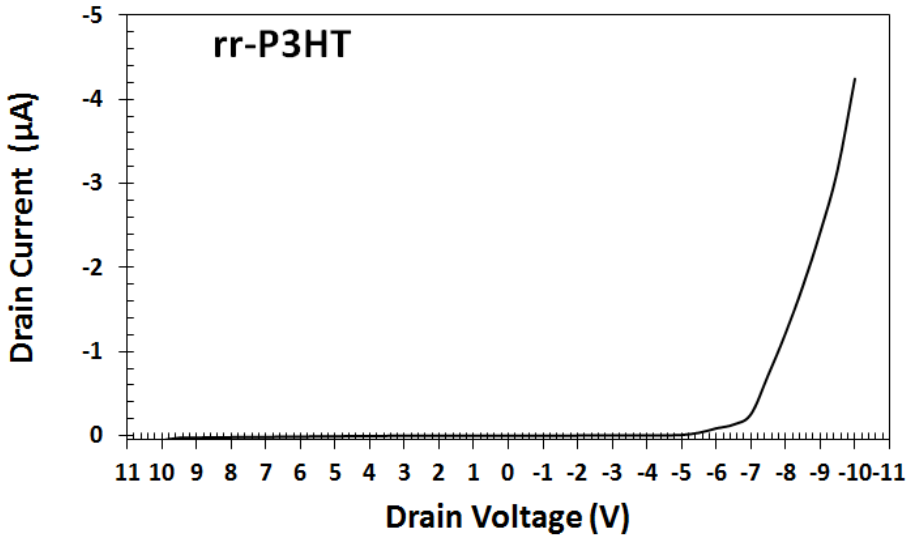

Figure 3.24. Diode characteristic of the synthesized rr-P3HT

3.6. OFET with 2 µm Technology

To be able to characterize the synthesized rr-P3HT and increase the performance of the lateral gated electrode system, it is necessary to build a channel with lower length. However, ordinary mask printing system cannot reach under the resolution level of 30 µm.

Therefore, OFET electrode mask design with channel length of 2 μm is implemented on soda-lime glass masks with 2 μm resolution.

The photoresist PR1828 was not suitable for the lithography process of 2 micron resolution because of its high coating thickness. Thus, photoresist PR1805 is used which gives coating thickness about 0.7μm at 2000 rpm. Resist coated wafer is exposed to UV light for 35 seconds with hard contact lithography. Then it is developed in MF26A developer for 45 seconds. These are the optimum parameters in our system which has been found after many trials. The other parameters of the lithography process have remained the same. The microscope images of the formed electrodes are shown in Figure 3.25.

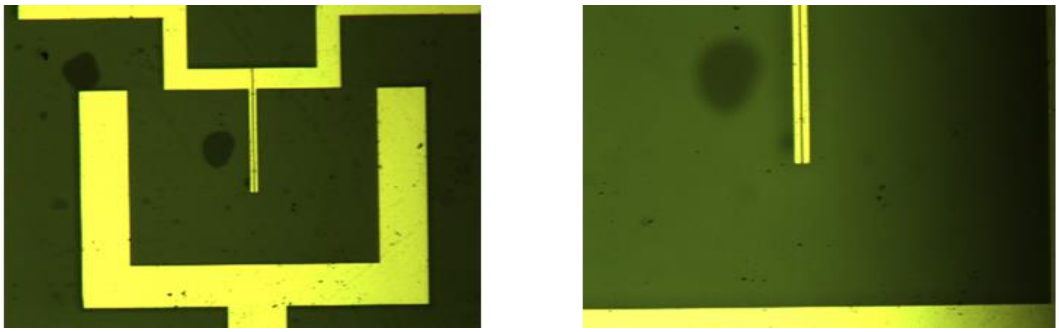

Figure 3.25. 2 μm electrode structure (left), closer view of channel (right)

The changed parameter in 2 micron structure is that the channel length becomes 4 μm and the width of the source-drain electrode legs become 15 μm. The reason for 4 μm length is the imperfections of the lithography process. As a result of this configuration W/L of the transistor is improved from 600/30=20 to 600/4=150.

After the functionality of the 2 μm OFET with synthesized rr-P3HT is shown, circuit structure of the new electrode system has been implemented to be able to use the functionalized polymers in circuit application. An extension mask is designed that connects the terminals between the individual transistors to implement the basic circuits explained in the previous sections. The L-Edit graph of circuit design and the extension mask is shown in Figure 3.26.

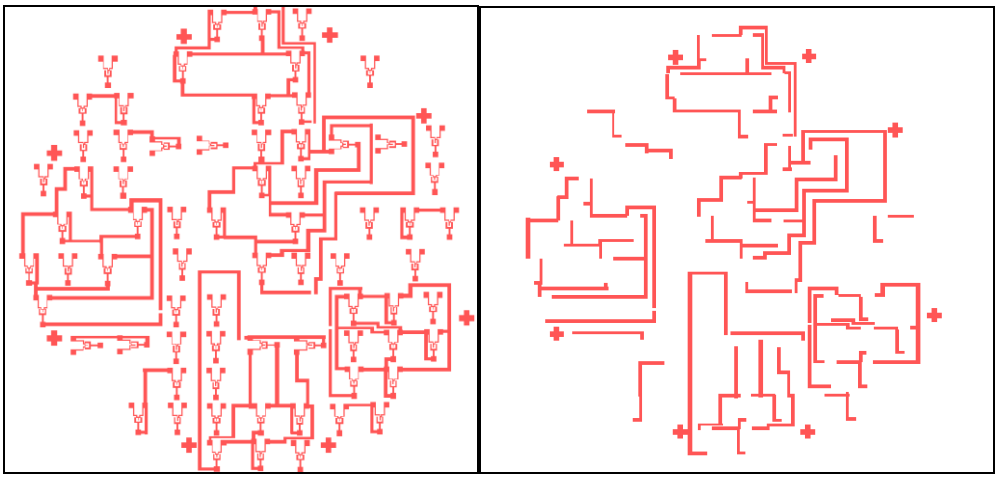

Figure 3.26. 2µm resolution electrode structure for circuit application (left), Extension mask of the 2µm resolution electrode mask

The extension mask is printed on a transparency with 30 µm resolution printer. Then, in order to form new electrode architecture two masks are aligned and they are stuck together with the help of capillary force of DI water. The image of the circuit electrode wafer is shown in Figure 3.27.

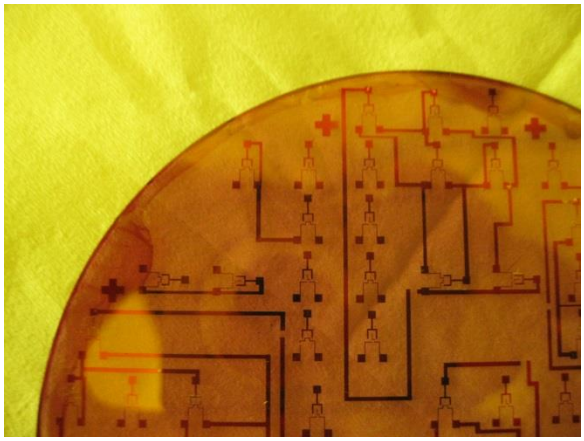

Figure 3.27. Image of the 2 µm electrode wafer for circuit application

3.7. Surface Roughness and Spin-Coating

In the experiments, we have observed that coating the P3HT solution to the surface of the wafer by spin-coating effectively enhances the water gated OFET characteristic compared to drop-casting. Even though, in the literature, it is claimed that drop-casting gives higher mobility hence better transistor performance, this claim is not relevant to our

case since our transistors have top gate contacts. These observations in the literature are for OFETs with bottom gate structure [54].

In water gated transistor structure, there is a great possibility that electrical double layer formation of the channel interface is disrupted by the surface roughness of the P3HT which is caused by the drop casting method. The microscope images showing the P3HT coated surfaces for both cases are given in Figure 3.28.

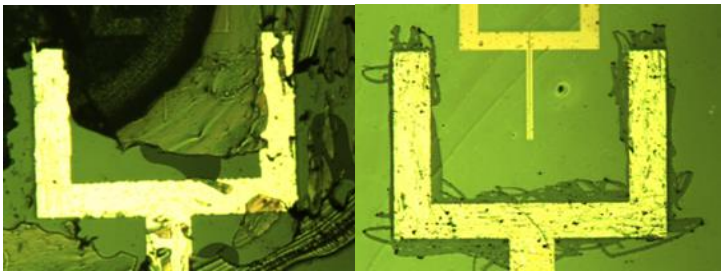

Figure 3.28. Microscope images of the P3HT coated electrodes
(left) Drop Casting Example, (right) Spin Coated OFET

Images clearly supports that surface uniformity is much better for spin-coated example. One drawback of the spin-coating is that once the wafer is spin coated, other transistors are also coated with P3HT. Thus, transistors are exposed to O_2 during the measurement of the other transistors. Additionally, spin-coating gives more surface area for oxidation. However, it is claimed that P3HT does not lose its functionality for a long time if it is sealed in a closed box [55]. This situation is corrected by observing transistor characteristic from coated P3HT, which was sealed a month ago.

Consequently, the developed fabrication steps are as following. P3HT solution is spin-coated at 2000 rpm. After this, it is leaved for annealing process inside a vacuum chamber for 1 hour in order to extract the solvent material and to improve the crystal structure of the conjugated polymer [56]. Image of spin coated P3HT is given in Figure 3.29.

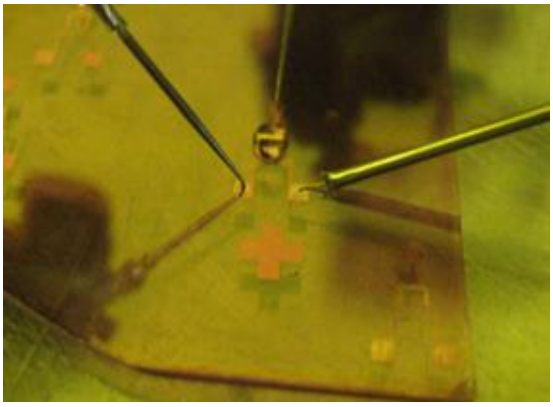

Figure 3.29. Water Gated OFET with Spin-Coated P3HT

3.8. P3HT-co-P3PEGT

Regio-regular P3HT is a hydrophobic material. Thus, the interface of rr-P3HT with aqueous solutions is poor. Hence, this behavior decreases the effect of electrical double layer capacitance of the aqueous solution. In order to change this situation, the chemistry division developed a functionalized P3HT, which has PEG molecules attached to some thiophene rings. As mentioned in earlier sections, PEG is a water soluble molecule. Thus, attaching PEG to the P3HT polymer increases the hydrophilicity of the polymer. Chain formulas of RR-P3HT and P3HT-co-P3PEGT are given in Figure 3.30.

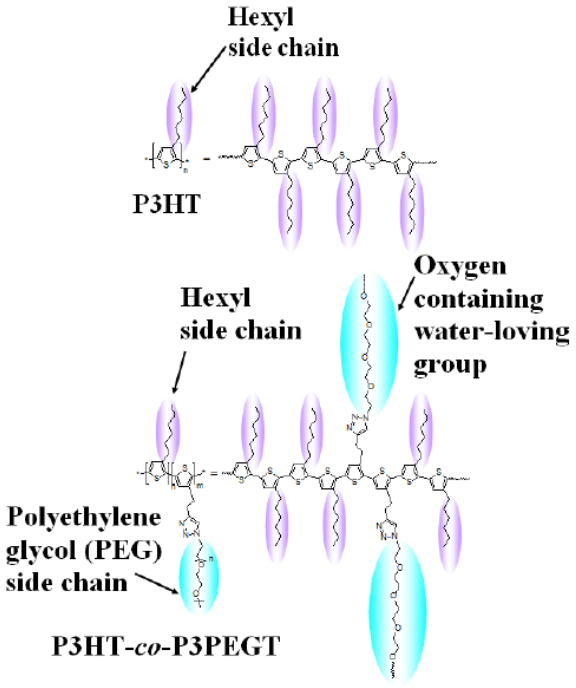

Figure 3.30. Rr-P3HT (up), P3HT-co-P3PEGT(bottom)

In order to prove the hydrophilicity of the synthesized P3HT-co-P3PEGT polymer, contact angle measurement is taken from both commercial P3HT and synthesized P3HT-co-P3PEGT. A water drop is put on to the surface of spin coated P3HT and P3HT-co-P3PEGT. The image of the contact angles are given in Figure 3.31.

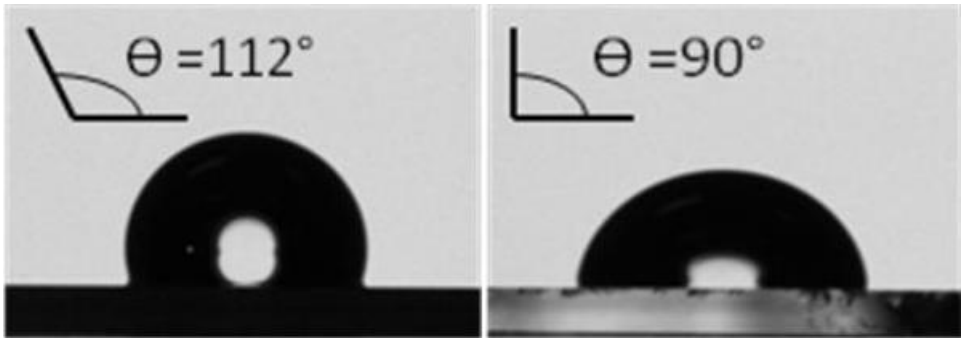

Figure 3.31. Contact Angle Measurement P3HT (left), P3HT-co-P3PEGT (right)

It can be seen that contact angle of water is smaller for the P3HT-co-P3PEGT coated surface which is a proof for hydrophilicity [57]. In the next chapter, OFET behavior of these polymers are examined.

4. RESULTS AND DISCUSSIONS

In this chapter, output results of several OFET examples are examined. Examining proceeds as comparison of results according to different control conditions. The aim is to find a suitable OFET fabrication condition to create a high gain inverter. However, there are many environmental conditions that affect the semiconductor polymer. Even for the transistors fabricated together on the same batch, experiments that are conducted at different time give different output results. Thus, every experiment should be considered in itself.

4.1. Transistor Comparisons

4.1.1. SiO_2 Insulated Bottom Gate Structure

The output result of Figure 4.1 is taken from the basic OFET structure as in Figure 2.4 where P3HT polymer is used as semiconductor polymer and SiO_2 is used for gate insulator [58]. As can be seen from the results, transistor needs 0 to 50V potential difference range for operation. This is not practical for many organic electronic applications. In the following examples it is shown that electrolyte gated OFET can achieve higher on currents with 0 to 1 V potential difference range.

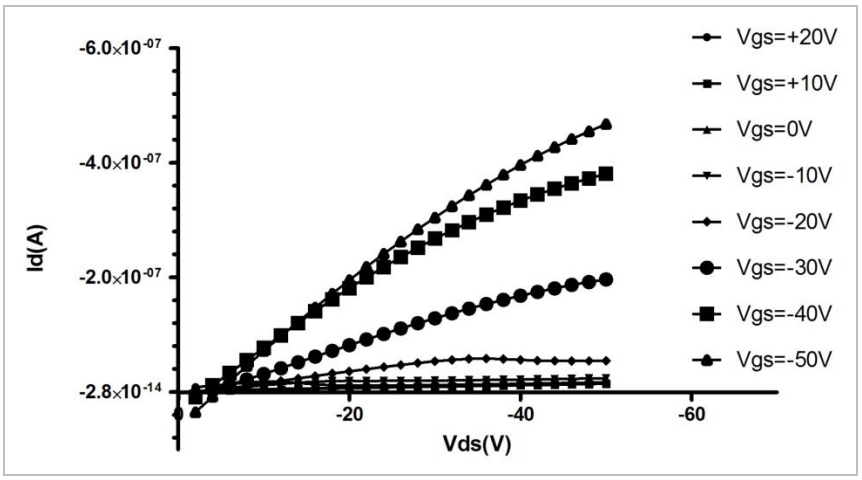

Figure 4.1. 200nm SiO_2 insulated Bottom Gate Structure [57]

4.1.2. 30 µm channel length vs. 2 µm channel length

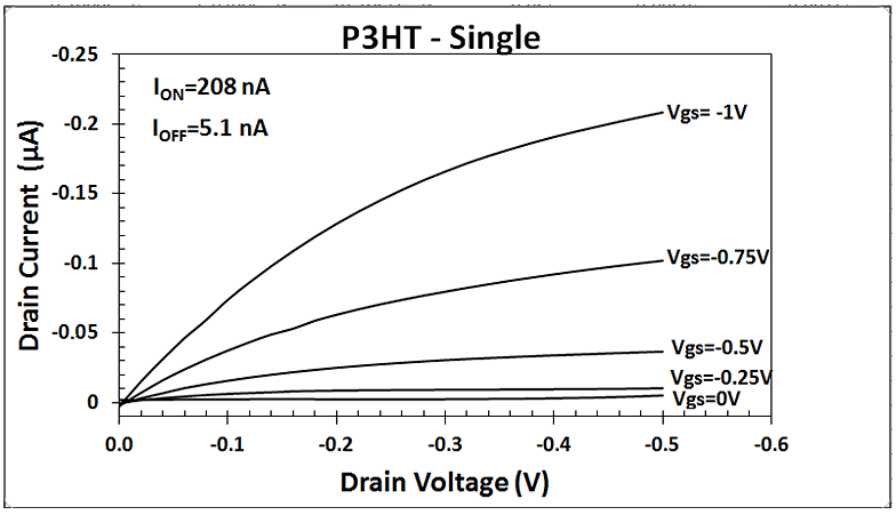

Figure 4.2. 30 µm channel I_D/V_{DS} output result (Parameters: Spin-Coated, DI water)

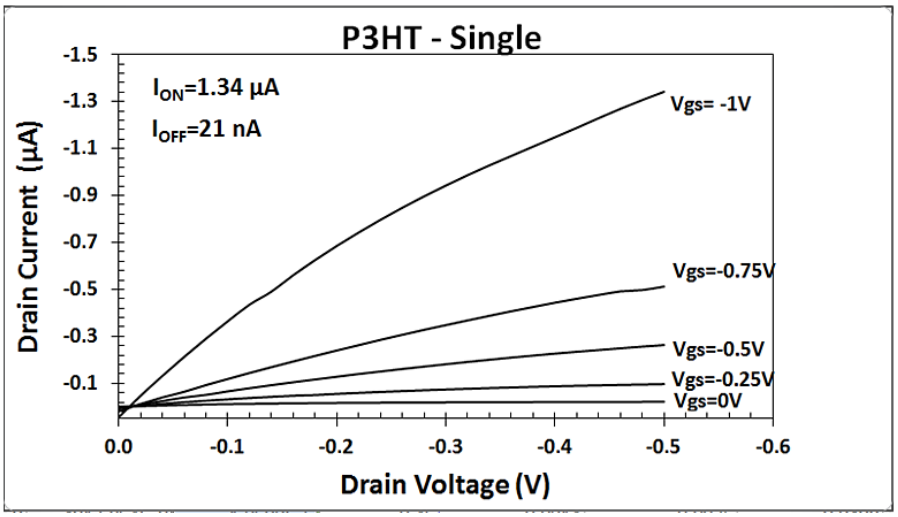

Figure 4.3. 4 µm channel I_D/V_{DS} output result (Parameters: Spin-Coated, DI water)

As we can see from the results that 4µm channel has better output performance. There is an important point that current-voltage curves of the 4µm channel transistor are very straight and they cannot show the effect of saturation. It can be explained by the dominating effect of contact resistance at short distance [59].

4.1.3. Drop-Casting vs. Spin-Coating

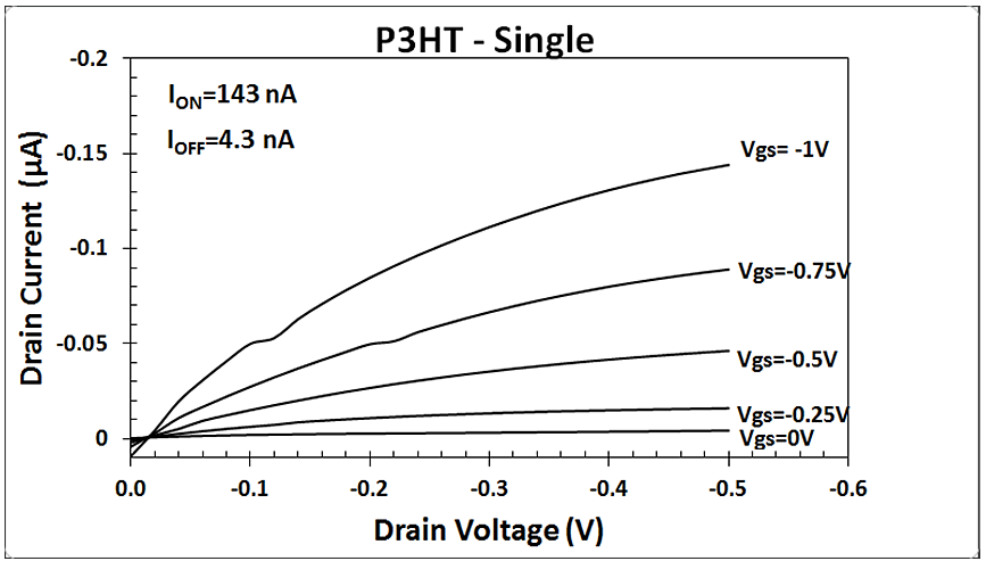

Figure 4.4. Drop-Casting I_D/V_{DS} output result (Parameters: 4µm channel, DI water)

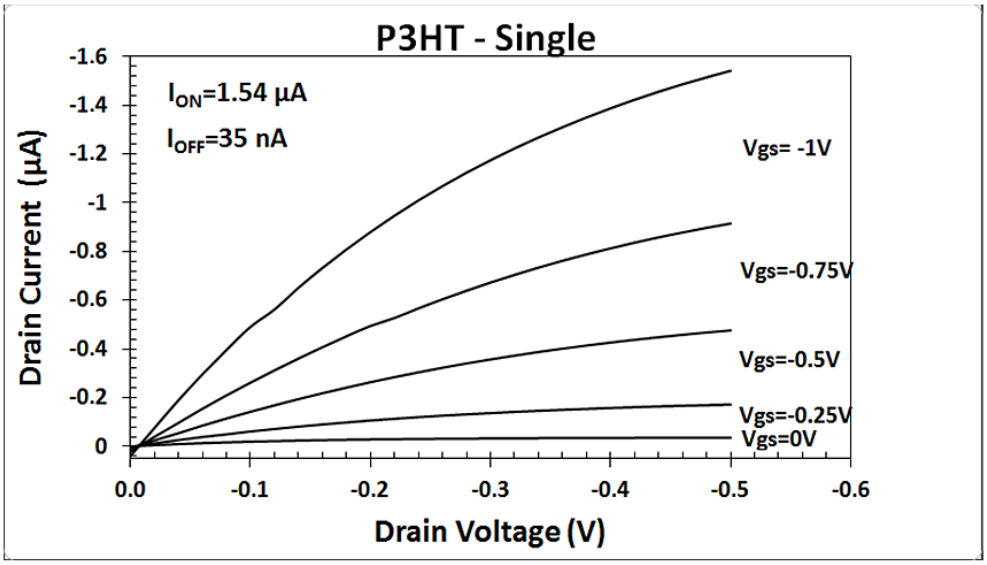

Figure 4.5. Spin-Coated I_D/V_{DS} output result (Parameters: 4µm channel, DI water)

As we can see from the results that OFET which is prepared with spin-coating has better output performance. These results proved that spin-coating must be employed and 4 µm channel length must be used in order to achieve better transistor performance. Therefore, these parameters are used for the following transistors. These are not mentioned explicitly in the following test results. The commercial P3HT has been used in the previous examples. In the next measurements, synthesized polymers are also tested for comparison.

4.1.4. Interdigitated P3HT

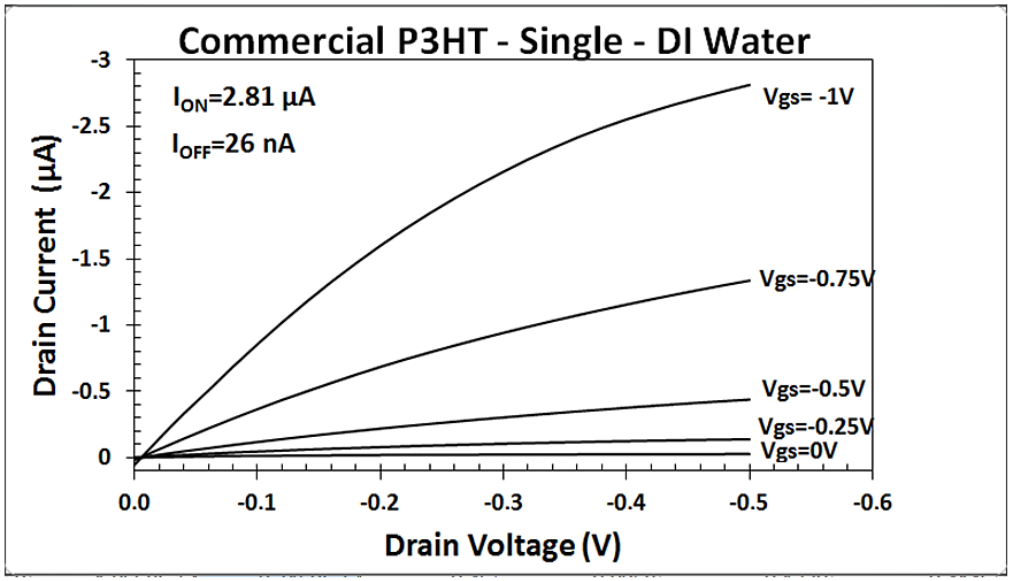

Figure 4.6. Single Structure I_D/V_{DS} output result (Parameters: DI water)

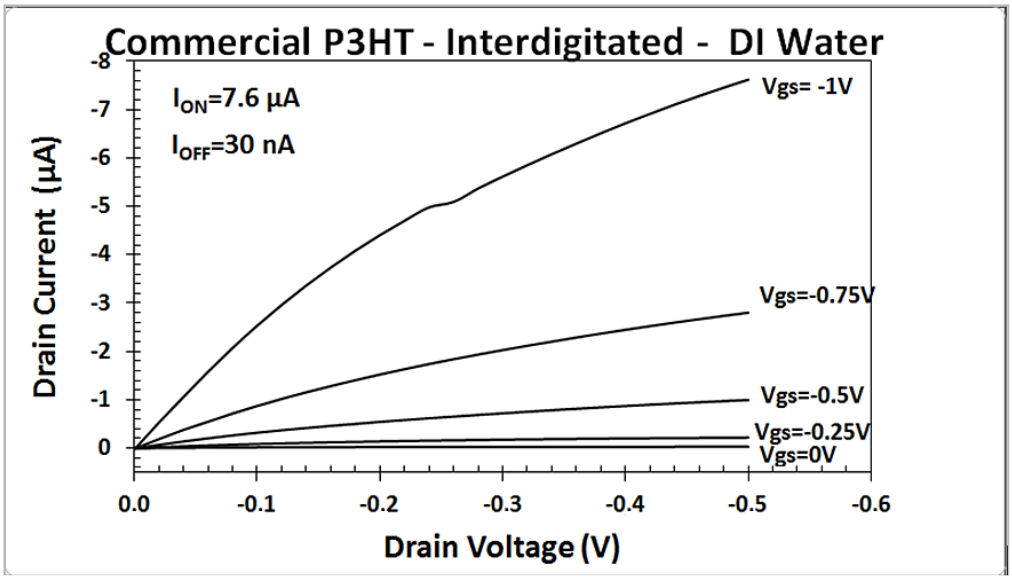

Figure 4.7. Interdigitated Structure I_D/V_{DS} output result (Parameters: DI water)

As can be seen in these results, interdigitated structure has more on current which provides better driving capability. It also gives flexibility for inverter design.

4.1.5. Synthesized P3HT and P3HT-co-P3PEGT

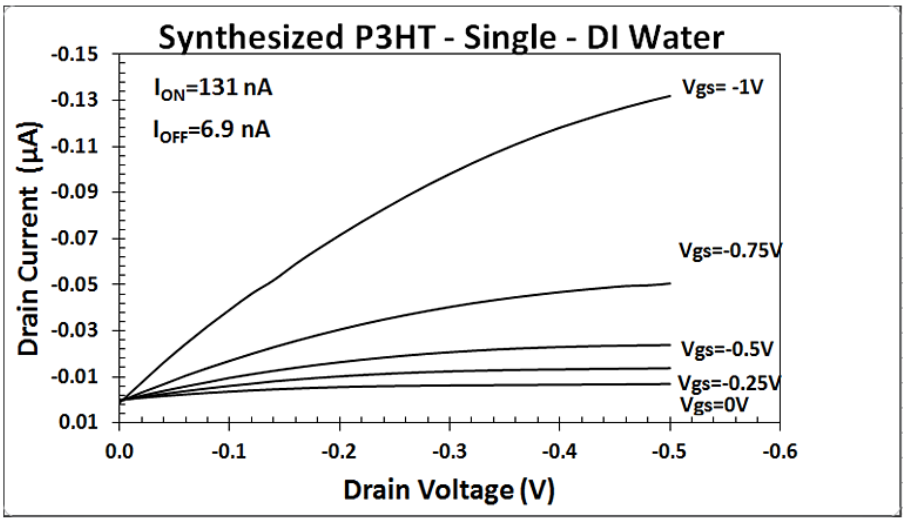

Figure 4.8. Synthesized P3HT I_D/V_{DS} output result (Parameters: DI water)

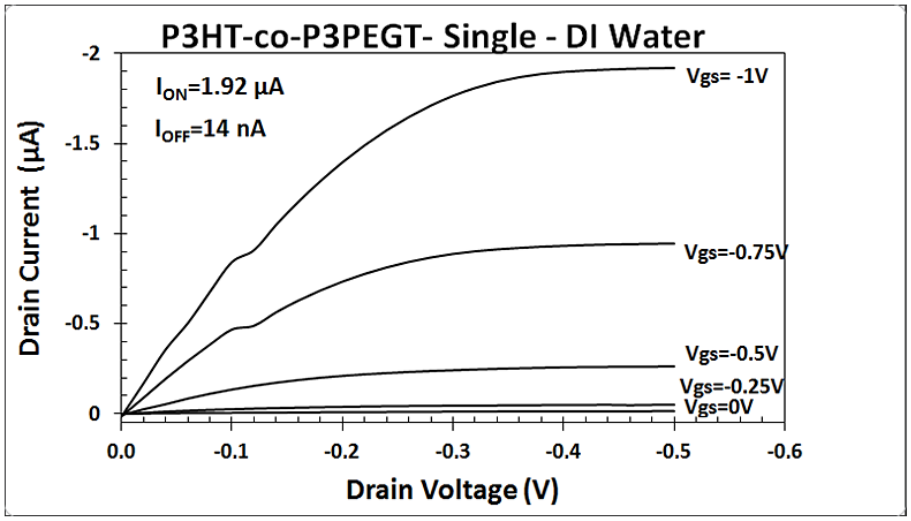

Figure 4.9. P3HT-co-P3PEGT I_D/V_{DS} output result (Parameters: DI water)

The output results of commercial P3HT and P3HT-co-P3PEGT are much better than the output result of the synthesized P3HT. Thus, commercial P3HT and P3HT-co-P3PEGT are taken into consideration in the next experiments.

4.1.6. I_D-V_{GS} Transfer Graph of Commercial P3HT and P3HT-co-P3PEGT

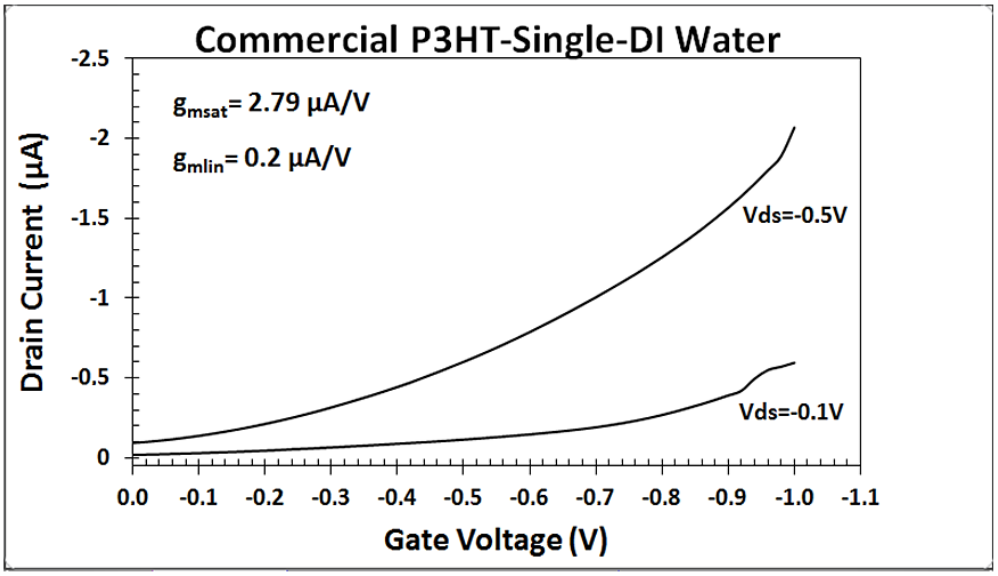

Figure 4.10. Commercial P3HT I_D/V_{GS} output result (Parameters: DI water)

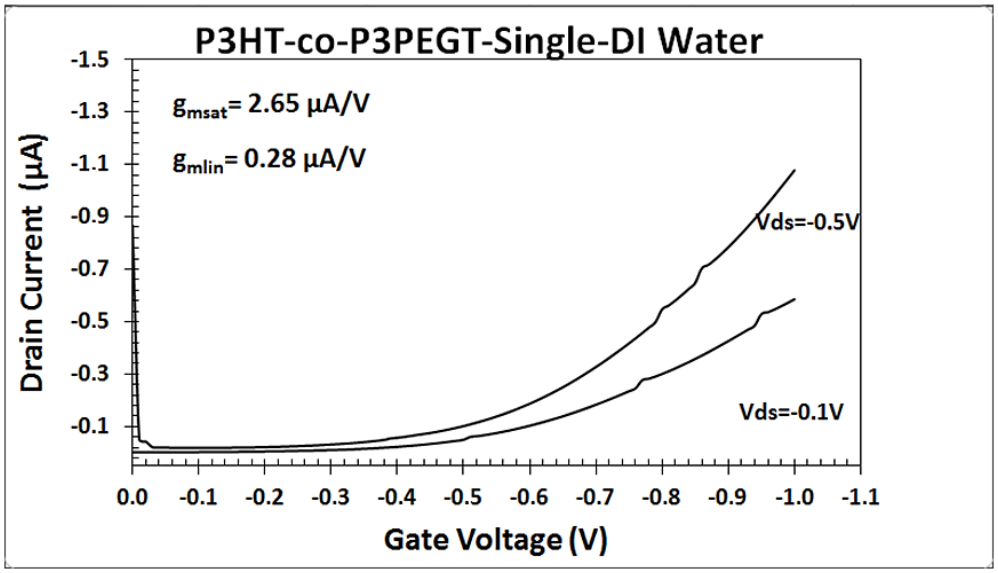

Figure 4.11. P3HT-co-P3PEGT I_D/V_{GS} output result (Parameters: DI water)

If we compare the results of the Figure 4.5 and 4.8, we see that at I_D/V_{GS} Graph on current of the same transistor reaches a current level (2.1µA) lower than the I_D/V_{DS} Graph (2.81µA). Same situation is also true for the P3HT-co-P3PEGT transistor. This situation implies that, the time needed for electrical double layer forming is a restrictive parameter for gate voltage sweep. Thus, I_D/V_{GS} graph is a crucial indicator showing the dependence of signal driving capability of the transistor on the response speed of gate voltage changes.

Transconductance (g_m) is an important parameter in order to drive the inverter with high speed and gain and g_m can be derived from the I_D/V_{GS} graph of the transistor. Thus, g_m is one of the main comparison criteria in the next transistors.

4.1.7. NaCl Solution as Gate Electrolyte

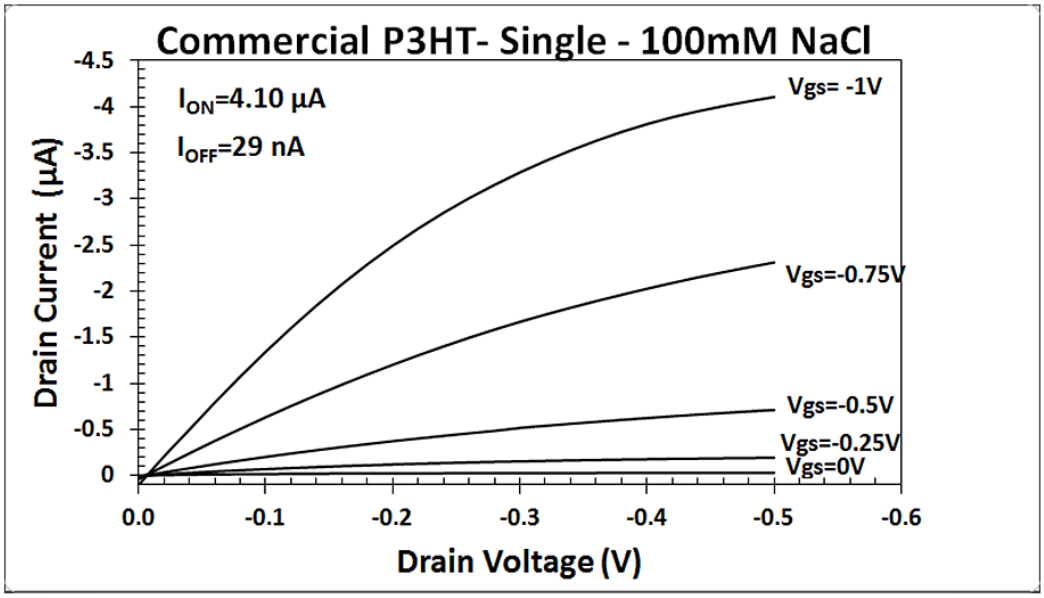

Figure 4.12. Commercial P3HT I_D/V_{DS} output result (Parameters: 100miliMolar NaCl solution)

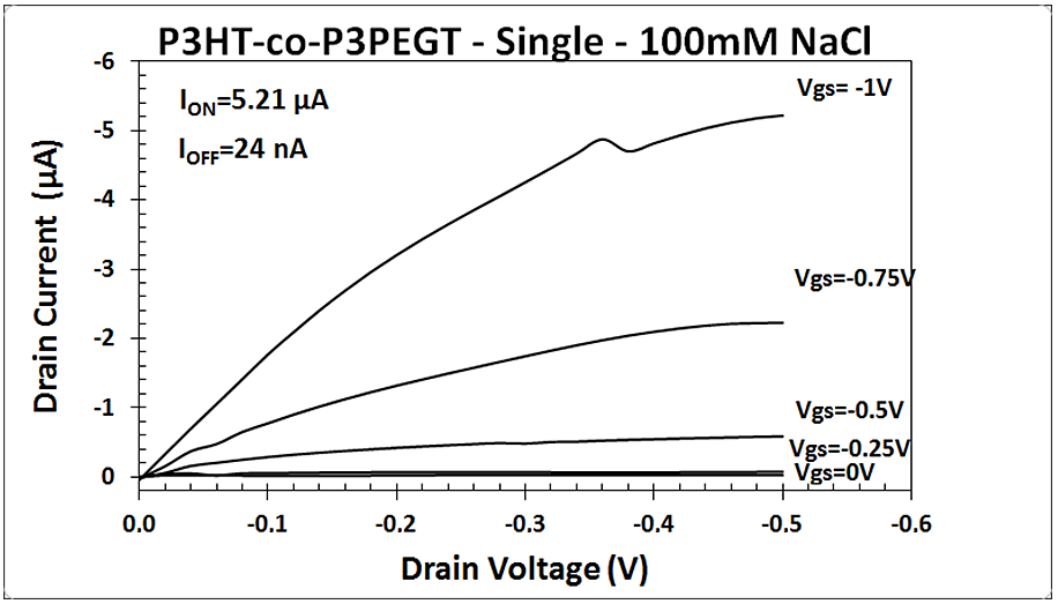

Figure 4.13. P3HT-co-P3PEGT I_D/V_{DS} output result (Parameters: 100miliMolar NaCl solution)

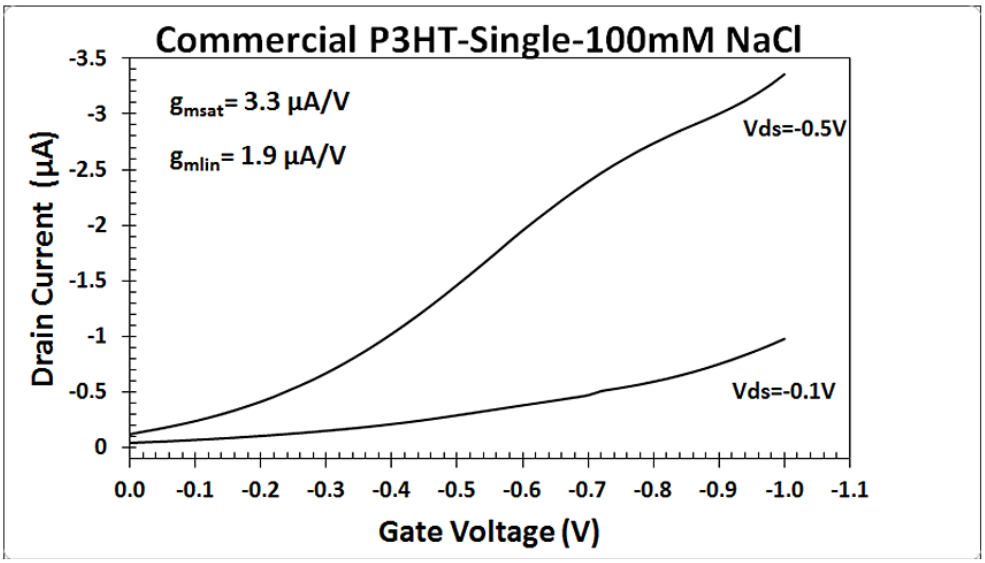

Figure 4.14. Commercial P3HT I_D/V_{GS} output result (Parameters: 100miliMolar NaCl solution)

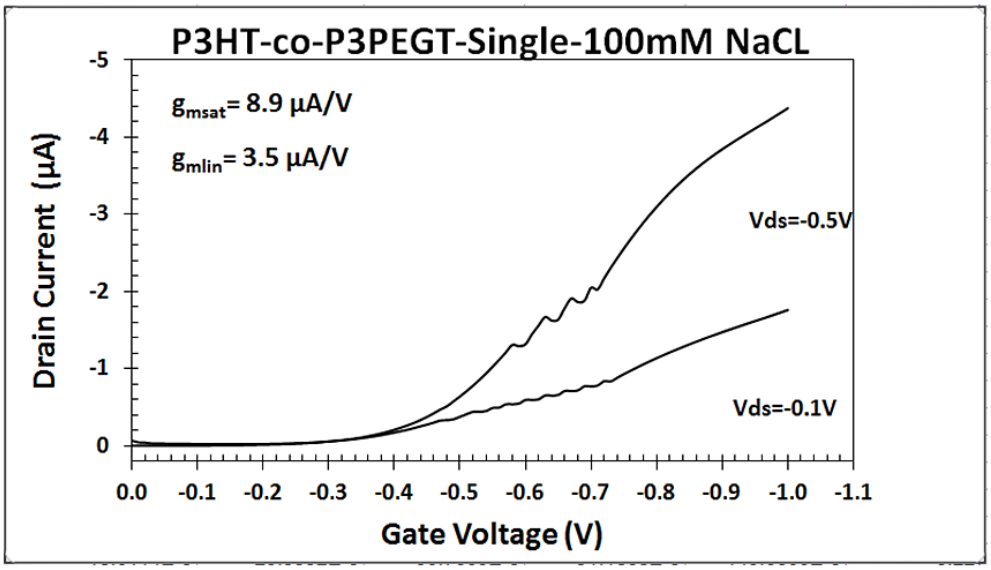

Figure 4.15. P3HT-co-P3PEGT I_D/V_{GS} output result (Parameters: 100miliMolar NaCl solution)

As we can see from these results, transconductance is increased for both polymers by the effect of the NaCl electrolyte, which is consistent with the theory saying that higher ionic concentration leads to faster polarization due to faster electrical double layer formation [49].

The more interesting part is that the change in transconductance of the P3HT-co-P3PEGT is much higher than the commercial P3HT. After these experiments, C-V measurements are done between the gate and the source of both transistors at 1 KHz. It is seen that for 100 miliMolar NaCl solution capacitance of the P3HT-co-P3PEGT transistor

was ten times higher in magnitude than the transistor with P3HT. This shows the importance of the hydrophilicity of the P3HT-co-P3PEGT polymer.

4.2. Inverter Comparisons

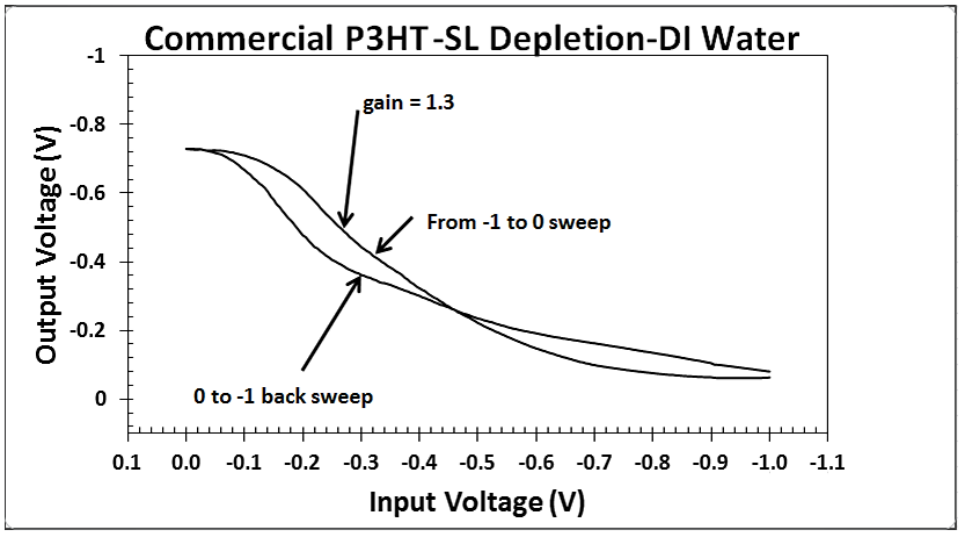

Figure 4.16. Commercial P3HT VTC (Parameters: Single-Interdigitated Inverter Electrode DI Water)

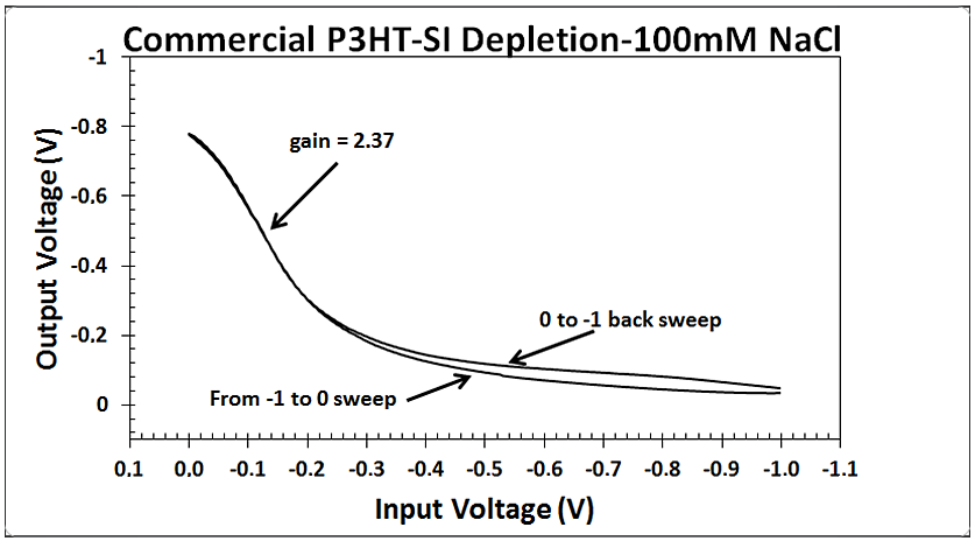

Figure 4.17. Commercial P3HT VTC (Parameters: Single-Interdigitated Inverter Electrode 100miliMolar NaCl solution)

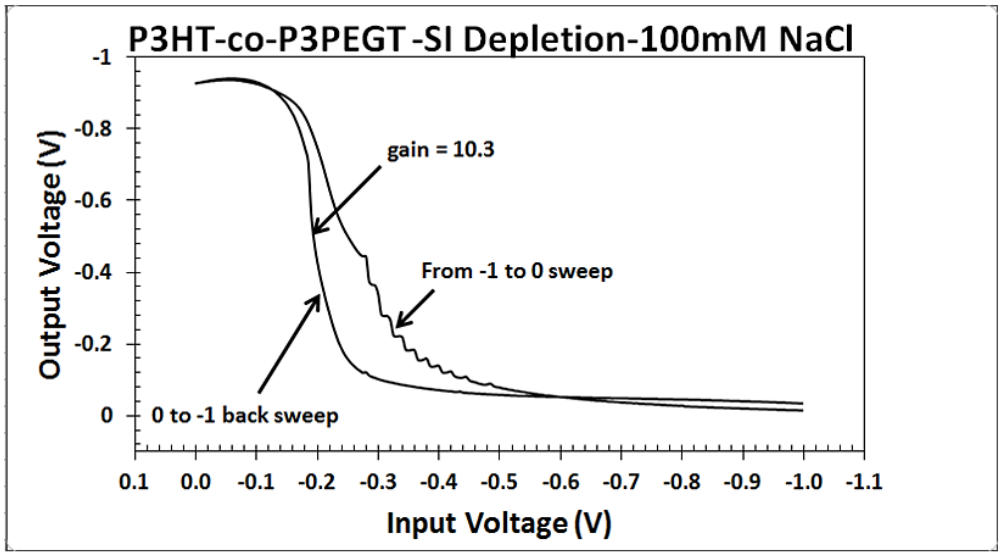

Figure 4.18. P3HT-co-P3PEGT VTC (Parameters: Single-Interdigitated Inverter Electrode 100miliMolar NaCl solution)

As can be seen from these results, NaCl solution increases the gain of the same inverter. In addition, P3HT-co-P3PEGT inverter has yielded very high gain for the electrolyte solution. The reason of the hysteresis effect may be electrochemical doping of P3HT-co-P3PEGT.

5. CONCLUSION AND FUTURE WORK

In this study, electrolyte gated OFET is implemented by a novel design which is named planar gate electrode design. Transconductance of the transistor is heightened by the effects of higher concentration in aqueous solution and hydrophilicity of the P3HT. Then, it is proved that OFET is convenient for circuit applications by building a high gain inverter where P3HT-co-P3PEGT used as semiconductor and 100 mM NaCl solution utilized as gate electrolyte.

In the next stage, the aim of the project will be building an oscillator from the electrolyte gated OFET. However there is one issue that the thin film of P3HT-co-P3PEGT is not resistant to aqueous solutions. This situation can be solved by adjusting the ratio of PEG molecule in the polymer chain. In addition, another research can be done on the concentration ratio of the aqueous solution to find the safe operating region for field effect transistor.

REFERENCES

1. Herlogsson L., *Electrolyte-Gated Organic Thin-Film Transistors,* Ph.D. Thesis, Linköping Studies in Science and Technology, 2011.

2. Said E., *Electrolyte-Based Organic Electronic Devices,* Lic. Thesis, Linköping Studies in Science and Technology, 2007.

3. Chang, J.B., V. Liu, V. Subramanian, K. Sivula, C. Luscombe, A. Murphy, J. Liu and J.M.J. Fréchet, "Printable polythiophene gas sensor array for low-cost electronic noses", *Journal of Applied Phys*ics, Vol. 100, 014506, 2006.

4. Laiho, A., L. Herlogsson, R. Forchheimer, X. Crispin and M. Berggren, "Controlling the dimensionality of charge transport in organic thin-film transistors", *Proceedings of the National Academy of Sciences*, Vol. 108, No. 37, pp. 15069–15073, 2011.

5. Comiskey, B., J.D. Albert, H. Yoshizawa, and J. Jacobson "An Electrophoretic Ink for All-Printed Reflective Electronic Displays", *Nature*, Vol. 394, No. 6690, pp. 253-255, 1998.

6. Ameri, T., G. Dennler, C. Lungenschmied, and C.J. Brabec, "Organic tandem solar cells: A review", *Energy and Environmental Science*, Vol. 2, No. 4, pp. 347–363, 2009.

7. Said, E., O. Larsson, M. Berggren, and X. Crispin, "Effects of the Ionic Currents in Electrolyte-gated Organic Field-Effect Transistors", *Advanced Functional Materials*, Vol. 18, pp. 3529–3536, 2008.

8. Kim, M., H. Cho, J. Kwak, C. Kang, M. Park and C. Lee, "Organic complementary inverter and ring oscillator on a flexible substrate", *Journal of Information Display*, Vol. 12, No. 1, pp. 1–4, 2011.

9. Boehm, M., A. Ullmann, D. Zipperer, A. Knobloch, W. H. Glauert and W. Fix, "Printable Electronics for Polymer RFID Applications", *IEEE International Solid-State Circuits Conference 2006*, Session 15.1, 2006.

10. Herlogsson, L., M. Colle, S. Tierney, X. Crispin and M. Berggren, "Low-Voltage Ring Oscillators Based on Polyelectrolyte-Gated Polymer Thin-Film Transistors", *Advanced Materials*, Vol. 22, pp. 72–76, 2010.

11. Klauk, H., U. Zschieschang and M. Halik, "Microcontact-Printed Self-Assembled Monolayers as Ultrathin Gate Dielectrics in Organic Thin-Film Transistors and Complementary Circuits", *Journal of Applied Phys*ics, Vol. 102, 074514, 2007.

12. Xia Y., W. Zhang, M. Ha, J.H. Cho, M.J. Renn, C.H. Kim and C.D. Frisbie, "Printed Sub-2 V Gel-Electrolyte-Gated Polymer Transistors and Circuits", *Advanced Functional Materials*, Vol. 20, pp. 587–594, 2010.

13. Panzer, M.J. and C.D. Frisbie, "Exploiting Ionic Coupling in Electronic Devices: Electrolyte-Gated Organic Field-Effect Transistors", *Advanced Materials*, Vol. 20, pp. 3177–3180, 2008.

14. Gebauer, P., *"*Pete Gebauer's Home Page Monmouth College*"*, http://personal.monm.edu/gebauer_peter/ CHEM_230/C230_index.htm, January 2013.

15. Heeger, A.J., "Semiconducting and Metallic Polymers The Fourth Generation of Polymeric Materials", *Angewandte Chemie International Edition*, Vol. 40, pp. 2591-2611, 2001.

16. Yuen, J.D., A.S. Dhoot, E.B. Namdas, N.E. Coates, M. Heeney, I. McCulloch, D. Moses and A.J. Heeger "Electrochemical Doping in Electrolyte-Gated Polymer Transistors", *Journal of the American Chemical Society*, Vol. 129, pp. 14367-14371, 2007.

17. Lee, J., L.G. Kaake, J.H. Cho, X.Y. Zhu, T.P. Lodge and C.D. Frisbie, "Ion Gel-Gated Polymer Thin-Film Transistors: Operating Mechanism and Characterization of Gate Dielectric Capacitance, Switching Speed, and Stability", *The Journal of Physical Chemistry C*, Vol. 113, No. 20, 2009.

18. Kaneto, K., T. Asano, and W. Takashima, "Memory Device Using a Conducting Polymer and Solid Polymer Electrolyte", *Japanese Journal of Applied Physics*, Vol. 30, L215, 1991.

19. Joshi, S., P. Pingel, S. Grigorian, T. Panzner, U. Pietsch, D. Neher, M. Forster and U. Scherf, "Bimodal Temperature Behavior of Structure and Mobility in High Molecular Weight P3HT Thin Films", *Macromolecules*, Vol. 42, No. 13, 2009.

20. Shimotani, H., G. Diguet and Y. Iwasa, "Electrolyte-gated charge accumulation in organic single crystals", *Applied Physics Letters*, Vol. 86, 022104, 2005.

21. Xia, Y., J.H. Cho, J. Lee, P.P. Ruden, and C.D. Frisbie, "Comparison of the Mobility–Carrier Density Relation in Polymer and Single-Crystal Organic Transistors Employing Vacuum and Liquid Gate Dielectrics", *Advanced Materials*, Vol. 21, pp. 2174–2179, 2009.

22. Skotheim, T.A. and J. Reynolds, *Handbook of Conducting Polymers*, 3rd Edition, CRC Press, New York, 2007.

23. Sirringhaus, H., P.J. Brown, R.H. Friend, M.M. Nielsen, K. Bechgaard, B.M.W. Langeveld-Voss, A.J.H. Spiering, R.A.J. Janssen, E.W. Meijer, P. Herwig and D.M. Leeuw, "Two-dimensional charge transport in self-organized, high-mobility conjugated polymers", *Nature*, Vol. 401**,** pp**.** 685-688, 1999.

24. Kline, R.J., M.D. McGehee, E.N. Kadnikova, J. Liu and J.M.J. Fréchet, "Controlling the Field-Effect Mobility of Regioregular Polythiophene by Changing the Molecular Weight", *Advanced Materials*, Vol. 15**,** pp. 1519-1522, 2003.

25. Zen, A., J. Pflaum, S. Hirschmann, W. Zhuang, F. Jaiser, U. Asawapirom, J.P. Rabe, U. Scherf and D. Neher, "Effect of Molecular Weight and Annealing of Poly(3-hexylthiophene)s on the Performance of Organic Field-Effect Transistors", *Advanced Functional Materials*, Vol. 14, No. 8, 2004.

26. Abdou, M.S.A., F.P. Orfino, Y. Son and S. Holdcroft, "Interaction of Oxygen with Conjugated Polymers: Charge Transfer Complex Formation with Poly(3-alkylthiophenes)", *Journal of the American Chemical Society*, Vol. 119, pp. 4518-4524, 1997.

27. Bard E. and L. Faulkner, *Electrochemical Methods: Fundamentals and Applications*, Wiley, New York, 2001.

28. Mirtaheri, P., S. Grimnes and Ø. G. Martinsen, "Electrode Polarization Impedance in Weak NaClAqueous Solutions", *IEEE Transactions on Biomedical Engineering*, Vol. 52, No. 12, 2005.

29. Marcilla, R., F. Alcaide, H. Sardon, J.A. Pomposo, C. Pozo-Gonzalo and D. Mecerreyes, "Tailor-made polymer electrolytes based upon ionic liquids and their application in all-plastic electrochromic devices", *Electrochemistry Communications*, Vol. 8, pp. 482-488, 2006.

30. Prigogine, I. and S.A. Rice, *Advances in Chemical Physics, Volume 94, Polymeric Systems*, Wiley, 2007.

31. Bordi, F., C. Cametti and R.H. Colby, "Dielectric spectroscopy and conductivity of polyelectrolyte solutions", *Journal of Physics: Condensed Matter*, Vol. 16, pp. R1423-R1461, 2004.

32. Lee, K., J. Park and H. Kim, "Ion Conductivity Studies of Blends of Poly(methy1 methacrylate)-g-Poly(ethy1ene glycol) and Poly(ethy1ene glycol) Complexed with LiCF3S03", *Journal of Polymer Science: Part B: Polymer Physics*, Vol. 34, pp. 1427-1433, 1996.

33. Kao, M.J., D.C. Tien, C.S. Jwo and T.T. Tsung, “The study of hydrophilic characteristics of ethylene glycol”, *Journal of Physics: Conference Series*, Vol. 13, pp. 442–445, 2005.

34. Wang, T., Y. Qi, J. Xu, X. Hu and P. Chen, “Effects of poly(ethylene glycol) on electrical conductivity of poly(3,4 ethylenedioxythiophene)–poly (styrenesulfonic acid) film”, *Applied Surface Science*, Vol. 250, pp. 188–194, 2005.

35. Meijer, E.J. and E. Cantatore, "Transistor Operation and Circuit Performance in Organic Electronics", *IEEE Transactions on Electron Devices*, Vol. 48, pp. 29-36, 2003.

36. Klauk, H., “Organic thin-film transistors”, *Chemical Society Reviews*, Vol. 39, pp. 2643–2666, 2010.

37. Shim, C., F. Maruoka and R. Hattori, “Structural Analysis on Organic Thin-Film Transistor with Device Simulation”, *IEEE Transactions on Electron Devices*, Vol. 57, No. 1, 2010.

38. Shimotani, H., H. Asanuma, J. Takeya and Y. Iwasa, “Electrolyte-gated charge accumulation in organic single crystals”, *Applied Physics Letters*, Vol. 89, 203501, 2006.

39. Hirahara, R., S. Ono, S. Seki, Y. Tominari and J. Takeya, “Organic Single Crystal Transistors Gated by Electric Double Layers in Ionic Liquid”, *Materials Research Society Symposium Proceedings*, Vol. 1091, 2008.

40. Kergoat, L., B. Piro, M. Berggren, G. Horowitz and M. Pham, “Advances in organic transistor-based biosensors: from organic electrochemical transistors to electrolyte-gated organic field-effect transistors”, *Analytical and Bioanalytical Chemistry*, Vol. 402, pp. 1813-1826, 2011.

41. Thackeray, J.W. and M.S. Wrighton, "Chemically responsive microelectrochemical devices based on platinized poly(3-methylthiophene): variation in conductivity with variation in hydrogen, oxygen, or pH in aqueous solution", *Journal of Physical Chemistry*, Vol. 90, pp. 6674–6679, 1986.

42. Cicoira, F., M. Sessolo, O. Yaghmazadeh, J.A. DeFranco, S.Y. Yang and G.G. Malliaras, "Influence of Device Geometry on Sensor Characteristics of Planar Organic Electrochemical Transistors", *Advanced Materials*, Vol. 22, pp. 1012–1016, 2010.

43. Ono, S., K. Miwa, S. Seki and J. Takeya, "A comparative study of organic single-crystal transistors gated with various ionic-liquid electrolytes", *Applied Physics Letters*, Vol. 94, 063301, 2009.

44. Larsson, O., E. Said, M. Berggren and X. Crispin, "Insulator Polarization Mechanisms in Polyelectrolyte Gated Organic Field-Effect Transistors", *Advanced Functional Materials*, Vol. 19, pp. 3334–3341, 2009.

45. Panzer, M.J. and C.D. Frisbie, "Polymer Electrolyte-Gated Organic Field-Effect Transistors: Low-Voltage, High-Current Switches for Organic Electronics and Testbeds for Probing Electrical Transport at High Charge Carrier Density", *Journal of the American Chemical Society*, Vol. 129, pp. 6599-6607, 2007**.**

46. Kergoat, L., L. Herlogsson, D. Braga, B. Piro, M.Pham, X. Crispin, M. Berggren and G. Horowitz, "A Water-Gate Organic Field-Effect Transistor", *Advanced Materials*, Vol. 22, pp. 2565–2569, 2010.

47. Kergoat, L., B. Piro, M. Berggren, M. Pham, A. Yassar and G. Horowitz, "DNA detection with a water-gated organic field-effect transistor", *Organic Electronics*, Vol. 13, pp. 1–6, 2012.

48. Mabeck, J.T., J.A. DeFranco, D.A. Bernards, G.G. Malliaras and S. Hocdé, "Microfluidic gating of an organic electrochemical transistor", *Applied Physics Letters*, Vol. 87, 013503, 2005.

49. Shimotani, H., G. Diguet and Y. Iwasa, "Direct comparison of field-effect and electrochemical doping in regioregular poly(3-hexylthiophene)", *Applied Physics Letters*, Vol. 86, 022104, 2005.

50. Someya, T., A. Dodabalapur, A. Gelperin, H.E. Katz, Z. Bao, "Integration and Response of Organic Electronics with Aqueous Microfluidics", *Langmuir***,** Vol. 18, pp. 5299-5302, 2002.

51. Cantatore, E., T.C.T. Geuns, G.H. Gelinck, E. van Veenendaal, A.F.A. Gruijhuijsen, L. Schrijenemakers, S. Drews and D.M. Leeuw, "A 13.56 MHz RFID System Based on Organic Transponders", *IEEE Journal of Solid-State Circuits*, Vol. 42, No. 1, 2007.

52. Xia, Y., W. Zhang, M. Ha, J.H. Cho, M.J. Renn, C.H. Kim and C.D. Frisbie, "Printed Sub-2 V Gel-Electrolyte-Gated Polymer Transistors and Circuits", *Advanced Functional Materials*, Vol. 20, pp. 587–594, 2010.

53. Raja, M., N. Sedghi, S. Badriya, S.J. Higgins, G.C.R. Lloyd and W. Eccleston, "Modelling of polymer Schottky diodes for real device applications", *Proceedings of ESSDERC*, Grenoble, France, 2005.

54. Austin, M.D. and S.Y. Chou, "Fabrication of 70 nm channel length polymer organic thin-film transistors using nanoimprint lithography", *Applied Physics Letters*, Vol. 81, pp. 4431-4433, 2002.

55. Ficker, J., A. Ullmann, W. Fix, H. Rost and W. Clemens, "Stability of polythiophene-based transistors and circuits", *Journal of Applied Phys*ics, Vol. 94, pp. 2638-2641, 2003.

56. Hao, X.T., T. Hosokai, N. Mitsuo, S. Kera, K.K. Okudaira, K. Mase and N. Ueno, "Control of the Interchain ð-ð Interaction and Electron Density Distribution at the Surface of Conjugated Poly(3-hexylthiophene) Thin Films", *The Journal of Physical Chemistry B*, Vol. 111, pp. 10365-10372, 2007.

57. Robinson, L., J. Isaksson, N.D. Robinson and M. Berggren, "Electrochemical control of surface wettability of poly(3-alkylthiophenes)", *Surface Science,* Vol. 600, pp. L148–L152, 2006.

58. Mert, O., *Fabrication and Testing of Polymer Thin Film Transistors for Basic Digital Circuits*, M.S. Thesis, Bogazici University, 2009.

59. Mas-Torrent, M., D. Boer, M. Durkut, P. Hadley and A.P.H.J. Schenning, "Field effect transistors based on poly(3-hexylthiophene) at different length scales", *Nanotechnology*, Vol. 15**.** pp. S265–S269, 2004.